CAHIER D'ÉTUDES
WORKING PAPER

N° 205

The Rich, the Poor, and the Carbon Tax

PABLO GARCIA SANCHEZ OLIVIER PIERRARD

MARCH 2026

BANQUE CENTRALE DU LUXEMBOURG
EUROSYSTÈME

THE RICH, THE POOR, AND THE CARBON TAX

PABLO GARCIA SANCHEZ AND OLIVIER PIERRARD

Abstract. Recent empirical evidence reveals an income gradient in support for climate action: individuals in wealthier countries are less willing to pay, as a percentage of their income, than those in poorer countries. What explains this gradient, and what does it imply for international cooperation to protect the Earth's climate? We answer these questions using a heterogeneous-country integrated assessment model formulated as a mean field game and calibrated to historical economic and climate data. Poorer countries, facing higher marginal utility of consumption, cut consumption less to cushion the decline in capital accumulation caused by climate damages. As a result, they suffer larger relative losses from climate change over time and gain more from mitigation, making them more inclined to accept a global carbon tax. This gradient has stark implications for cooperation: even when a carbon tax large enough to contain temperature increases benefits most countries, the richest might oppose. Redistributing global carbon tax proceeds uniformly across countries or recycling them as green investment subsidies need not overcome this reluctance.

JEL Codes: C61, H23, Q50.

Keywords: Neoclassical Growth Model; Mean Field Game; Climate Policy.

March 2026. Banque centrale du Luxembourg, Département Économie et Recherche, 2 boulevard Royal, L-2983 Luxembourg (contact: pablo.garciasanchez@bcl.lu, olivier.pierrard@bcl.lu).

Résumé Non Technique

Le changement climatique est un enjeu majeur pour les banques centrales, car il a des répercussions sur l'économie, et donc sur la stabilité des prix, la stabilité financière et la transmission de la politique monétaire. Conformément à son plan 2024-2025, la BCE a affiné son évaluation des risques liés au climat et à la nature, y compris la manière dont ils éclairent les décisions politiques.[1] Notre étude, qui vise à mieux modéliser l'évolution des émissions de CO_2 et leurs liens avec les politiques climatiques, s'inscrit pleinement dans ce cadre.

Plus précisément, cet article développe un modèle à plusieurs pays, qui combine une structure de croissance néoclassique avec un module climatique dans lequel la production génère du CO_2, qui s'accumule dans l'atmosphère et réduit la croissance. Ce modèle permet d'analyser une éventuelle taxe carbone au niveau mondial. En particulier, il permet d'identifier quels pays seraient en faveur d'une telle initiative et comment leur décision pourrait dépendre de l'horizon retenu.

Les paramètres du modèle sont calibrés à l'aide de données sur la production, le stock de capital et l'utilisation de l'énergie, portant sur plus de 130 pays, ainsi que sur les prix de l'énergie et la concentration de CO_2 atmosphérique au niveau mondial.

Trois principaux résultats se dégagent. Premièrement, limiter la hausse des températures nécessite une taxe carbone élevée. Par exemple, avec une taxe de \$351/tCO_2, l'augmentation de la température depuis 2021 serait limitée à 0.25°C en 2050 et 1.2°C en 2100.[2] Par contre, une taxe de seulement \$37/tCO_2 conduit à un réchauffement de 0.7°C en 2050 et de 3°C en 2100.

Deuxièmement, les pays riches sont moins enclins à adopter une taxe carbone que les pays pauvres, ce qui est cohérent avec les résultats d'enquêtes d'opinion auprès du public (Andre et al., 2024). Cette réticence s'explique par le fait que les pays riches sont plus aptes à s'adapter aux conséquences du changement climatique.

Troisièmement, l'intérêt pour une taxe carbone dépend également de l'horizon temporel retenu. En effet, à court terme, la taxe carbone ralentit la croissance économique, mais elle

[1] `https://www.ecb.europa.eu/press/pr/date/2026/html/ecb.pr260116~4b4a05a179.en.html`.

[2] A titre d'illustration, en 2024, la taxe carbone moyenne s'élevait à \$53 en Europe. Selon les pays, cette taxe ne s'applique qu'à certains types de gaz à effet de serre, ce qui ramène in fine la taxe moyenne effective plutôt aux alentours de \$25 (source: `https://taxfoundation.org/data/all/eu/carbon-taxes-europe-2024/`). Par ailleurs, une hausse des températures de 1.2°C depuis 2021 correspond à une hausse de 2.2°C par rapport à la période préindustrielle. Pour rappel, l'Accord de Paris, adopté en 2015, vise à maintenir l'augmentation de la température mondiale nettement en dessous de 2°C, par rapport à la période préindustrielle, et à poursuivre les efforts pour limiter la hausse à 1.5°C.

la stimule à plus long terme. Ce résultat reflète deux forces opposées. D'une part, la taxe accroît le prix des énergies fossiles, ce qui freine l'accumulation du capital. D'autre part, en réduisant les émissions mondiales de CO_2, la taxe accélère la croissance de la productivité, ce qui compense finalement l'effet négatif initial.

1. Introduction

Individuals in wealthier countries are less willing to pay a given share of income to fight climate change than those in poorer countries (Andre et al., 2024). This pattern is not limited to the extremes of rich and poor nations, but forms a gradient with per capita income (Figure 1). Two questions arise. First, what drives this gradient? Second, how does it shape (the lack of) international cooperation to address climate change?

We address these questions using a heterogeneous-country integrated assessment model, in the spirit of Hassler and Krusell (2012) and Hillebrand and Hillebrand (2019). The model combines a neoclassical growth structure with a climate block in which production generates CO_2 that accumulates in the atmosphere and hinders output growth (see Chang et al., 2023, for empirical evidence). We write the model in continuous time with a continuum of countries that differ in their initial capital stocks. This structure yields a mean field game (MFG) system with four equations. A backward Hamilton-Jacobi-Bellman (HJB) equation governs optimal consumption and saving choices, a forward transport equation describes the cross-sectional distribution of countries, and two ordinary differential equations determine atmospheric CO_2 and the global growth rate of labor and labor-augmenting productivity.[3] Framing the model as a MFG condenses an otherwise high-dimensional problem, enhances computational tractability and clarifies the underlying economic mechanisms.

We calibrate the model using data for 134 countries from 1990 to 2021 on production, capital stocks, and energy use, as well as global variables such as energy prices and atmospheric CO_2. The model aligns well with non-targeted moments, generating a large rise in median output per capita over the last three decades, together with a moderate increase in CO_2 emissions per capita and declining carbon intensity. It also captures key interactions, matching the increasing convex relationship between output and emissions across countries and the almost flat profile between carbon intensity and output per capita. The model replicates the rapid rise in atmospheric CO_2 too.

Our setup also predicts a negative cross-country correlation between the economic costs of climate change and national income levels, consistent with empirical evidence (see, e.g., Dell et al., 2012; Burke et al., 2015; Nath et al., 2024). Although rising atmospheric CO_2 concentrations lower the common growth rate of labor and labor-augmenting productivity, countries respond differently to this decline. High-income countries, which have a lower marginal utility of consumption, reduce current consumption to sustain capital accumulation. Lower-income countries, by contrast, have a higher marginal utility of consumption and are less willing to cut current consumption. As a result, capital accumulation declines more

[3] See Nath et al. (2024) for evidence that long-run output growth rates across countries are closely linked.

FIGURE 1. Willingness to contribute 1% of income by GDP

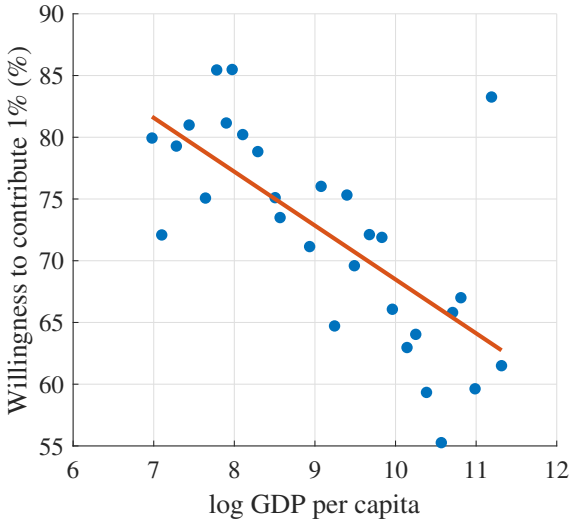

Notes. Binned scatter plot of the country-level proportion of individuals willing to contribute 1 percent of their income and 2021 log GDP per capita. The underlying data cover 108 countries, grouped into 30 bins. Data sources are listed in Appendix A.

sharply in poorer countries, generating a negative gradient in the economic costs of climate change across income levels.

With the model shown to align with a wide range of empirical regularities, we use it as a quantitative laboratory to evaluate the effects of a global carbon tax and countries' willingness to accept it. We anchor the carbon tax to the social cost of carbon estimates in Rennert et al. (2022), who report a point estimate of \$157 (2010 prices) per ton of CO_2, with a 95% confidence interval from \$37 to \$351. Our results show that keeping temperature increases within widely accepted bounds requires a carbon tax at the upper end of this range. A tax of \$351/tCO_2 limits the temperature increase since 2021 to about 0.25°C by 2050 and 1.2°C by 2100.[4] Instead, a low tax of \$37/tCO_2 allows substantially higher warming, around 0.7°C by 2050 and 3°C by 2100.

In line with Figure 1, our setup generates an income gradient in the willingness to accept climate action. When the effects of a \$351/tCO_2 carbon tax are evaluated over a horizon corresponding to the remaining lifetime of today's young adults, countries in the 5th percentile of the income per capita distribution (e.g., Madagascar) would be willing to forgo 0.9% of their consumption every instant to move from the baseline to the tax scenario. By contrast, countries in the 95th percentile (e.g., the United States) would require a 2.2% *increase* in their consumption to accept the same policy. This gradient arises because poorer

[4]Relative to 1850–1900 pre-industrial levels, these correspond roughly to 1.3°C and 2.2°C.

countries face larger economic damages from atmospheric CO_2 and therefore benefit more from protecting the Earth's climate.

Our exercises cast doubt on a common explanation for the income gradient in Figure 1, namely that it reflects higher adaptation costs in richer countries because they have higher CO_2 emissions (Andre et al., 2024). In our setup, richer countries do emit more CO_2, but emissions per unit of output are identical across countries, consistent with the almost flat relationship between carbon intensity and output in the data. Ceteris paribus, a given carbon tax entails the same output cost across countries. Hence, the income gradient in the willingness to accept climate action need not stem from higher mitigation or adaptation costs in rich countries, but from greater climate damages in poorer ones. Needless to say, we focus on economic mechanisms; other factors, such as geographic exposure to climate risks or political economy considerations, may also contribute to the observed gradient.

In addition, our policy experiments show that a country's willingness to adopt the carbon tax depends on its evaluation horizon. The tax has a non-monotonic effect on output growth, initially slowing it but boosting it over longer horizons. This results from two opposing forces. The tax raises fossil fuel prices, slowing capital accumulation similar to a negative productivity shock. Over time, however, it reduces global CO_2 emissions, accelerating the growth rate of labor and labor-augmenting productivity and eventually outweighing the initial drag. For example, over a 10-year horizon, no country would accept the $\$351/tCO_2$ tax, whereas over a 60-year horizon, all countries up to the 65th percentile would. As the horizon extends toward infinity, even the richest countries benefit: far-sighted countries at the top of the income distribution would forgo about 10% of their consumption to move from the baseline to the $\$351/tCO_2$ tax scenario.

These results show that the income gradient shapes international cooperation on climate policy and can make inaction rational for rich countries. Carbon tax schemes often discussed in public debates struggle to overcome this reluctance. One proposal redistributes global carbon tax revenues uniformly across countries rather than returning them domestically, which steepens the income gradient and weakens rich countries' incentives to adopt the tax. Another recycles revenues into subsidies for green capital investment. Although this increases support over long horizons, it reduces it in the short run by lowering consumption and utility. Overall, no simple policy design eliminates the short-run costs of abandoning fossil fuels across the income distribution.

Our effort builds on a growing literature that uses dynamic general equilibrium models to study the links between the macroeconomy and the climate. Because of the breadth of this field, we only review a few central contributions. And since our model is in real terms and focuses on long-run trends, we set aside the large literature on business-cycle effects of

global warming and the policies designed to address them (see e.g., Garcia et al., 2026, and references therein).

One major line of research studies climate policy in a closed-economy context. Seminal work by Golosov et al. (2014) provides an analytical formula for the optimal carbon tax, highlighting its dependence on the discount rate and the economic damages from emissions. Later studies, such as van den Bremer and van der Ploeg (2021), build on this foundation to show how uncertainties in the climate and the economy can shape the optimal tax rate. In related work, Acemoglu et al. (2012, 2016) incorporate endogenous economic growth, model the competition between clean and dirty technologies, and study the joint use of carbon taxes and research subsidies.

This line of research has also developed in multi-region settings. Hassler and Krusell (2012) use a four-region model to study how the welfare effects of carbon taxes differ both across and within oil-consuming and oil-producing regions. In another study, Hillebrand and Hillebrand (2019) develop a two-region model to study how the burden of climate change can be shared through transfer payments across countries. In later work, the same authors expand the analysis to six regions (Hillebrand and Hillebrand, 2023). In turn, Kotlikoff et al. (2024) adopt a similar framework but use an overlapping-generations structure to study carbon taxation and redistribution not only across countries but also across generations. Lastly, Hassler et al. (2025) develop a model with very high spatial resolution by dividing the globe into $1^\circ \times 1^\circ$ cells, highlighting large geographic dispersion in climate damages.

Our contribution to this literature is twofold. First, existing multi-region models are formulated in discrete time with a finite number of regions, which quickly leads to high numerical complexity. By contrast, we move to continuous time and model countries as a continuum. This formulation collapses the problem into a mean field game (MFG), as introduced to economics by Achdou et al. (2022). The resulting four-equation system is highly tractable and amenable to standard numerical methods. Second, to our knowledge, we present the first theoretical framework that studies the income gradient in the willingness to accept climate action, and analyzes its implications for international cooperation to fight global warming.

A paper using mathematical tools closer to ours is Aid et al. (2025), who study a mean field game in which firms' productivity is affected by temperature-driven damages linked to the global carbon stock. However, they focus on heterogeneity across firms in a closed economy, while we study heterogeneity across countries. In addition, their contribution is primarily theoretical, while ours takes a quantitative approach.

The remainder of the paper is organized as follows. Section 2 sets out the empirical regularities that guide our modeling approach. Section 3 presents the model. Section 4 describes the

solution method, and Section 5 maps the model to the data. Sections 6 and 7 present the main quantitative results, while Section 8 examines their robustness. Section 9 concludes.

2. Empirical Regularities

Although consistency with the data is not a sufficient condition, it is a necessary one for any model to serve as a reliable guide for policy analysis. Hence, this section presents several empirical regularities that will later be used to assess our model's quantitative performance. Only once we show that the model is in line with these patterns will we be confident in its ability to evaluate the quantitative effects of climate policy.[5]

The first three empirical regularities characterize the evolution of the components of the following identity

$$\text{Carbon intensity} = \frac{\text{CO}_2 \text{ emissions per capita}}{\text{Output per capita}},$$

between 1990 and 2021, both across a sample of 134 national economies and at the global aggregate level.[6]

Empirical regularity 1: Rising output per capita with persistent dispersion. Table 1 (columns '*Real output per capita*') shows that between 1990 and 2021, average output per capita across countries more than doubled, reflecting broad-based global economic growth. At the same time, standard deviation across countries grew proportionally with the mean, so that relative dispersion remained roughly constant. Moreover, the (right) skewness of the distribution was unchanged, indicating similar growth across the output distribution.

Empirical regularity 2: Stable CO_2 emissions per capita with persistent dispersion. CO_2 emissions per capita remained broadly stable over the same period. The mean fell slightly while the median rose, but the overall dispersion was largely unchanged, as reflected in similar values of the standard deviation and (right) skewness.

Empirical regularity 3: Declining carbon intensity with reduced dispersion. As a consequence of regularities 1 and 2, carbon intensity, or CO_2 emissions per unit of output, fell sharply, with the average declining by 55% and the median by 40%. In addition, the cross-sectional distribution became much more concentrated, as reflected in an 80% decline in the standard deviation.

Overall, these first three empirical patterns show that most countries met the decline in the left-hand side of the identity (carbon intensity) not by reducing the numerator (CO_2

[5]Although the selection of empirical regularities inevitably entails some judgment, we are confident that the chosen indicators are broad enough to capture the key interactions between growth and global warming over the past three decades.

[6]The time span of the historical sample is determined by data availability.

TABLE 1. Output per capita, CO_2 emissions per capita and carbon intensity in 1990 and 2021

	Real output per capita (1000 USD)		*CO_2 emissions per capita* (Tons)		*Carbon intensity* (Tons CO_2 per 1000 USD)	
	1990	2021	1990	2021	1990	2021
Mean	9.64	20.3	5.28	4.96	0.49	0.23
Median	6.1	12.9	2.34	2.78	0.30	0.19
Stand. dev.	9.42	21.3	6.78	6.61	0.58	0.13
Skewness	1.13	1.04	1.30	0.99	0.98	0.91

Notes. The table reports the first three moments and the median of the cross-sectional distributions of output per capita, CO_2 emissions per capita and carbon intensity, for 134 national economies in 1990 and 2021. All values in USD are expressed at 2011 price levels. Data sources are listed in Appendix A.

emissions per capita) but by increasing the denominator (output per capita). In addition, despite the rapid convergence of carbon intensity across countries, cross-country differences in both output and emissions per capita remain large.

A follow-up question emerges: how are the three variables in our basic identity linked across countries? Figure 2 addresses this question.

Empirical regularity 4: CO_2 emissions rise with output per capita, carbon intensity does not. CO_2 emissions per capita are strongly linked to output per capita, and this pattern has held over the past three decades. The gap is large: Figure 2 shows that countries at the 80th percentile emit 20 times as much CO_2 per capita as those at the 20th percentile. Instead, there is no clear link between carbon intensity and output per capita, especially in 2021, consistent with the low dispersion in carbon intensity noted above.

Because atmospheric CO_2 drives global warming, our final empirical regularities relate to atmospheric CO_2 and its implications on GDP.

Empirical regularity 5: Soaring atmospheric CO_2. Per capita levels of CO_2 emissions were roughly constant from 1990 to 2021, but the global population rose from 5.3 billion to 7.92 billion. As a result, total atmospheric CO_2 continued to rise, increasing by 18%.

Empirical regularity 6: Warming generates significant output losses, with disproportionate impacts on poorer countries. Nath et al. (2024) estimate that a warming of 3.7°C relative to pre-industrial levels would reduce global GDP by 8–13% by 2099, corresponding to an output loss of approximately 2.2 to 3.7% per degree of warming. Bilal and Kanzig (2024) find larger effects, estimating a reduction in world GDP exceeding 20% per degree of warming by 2100. Finally, Newell et al. (2021) show that rich countries, which have greater adaptive

FIGURE 2. CO_2 emissions and carbon intensity across the output distribution

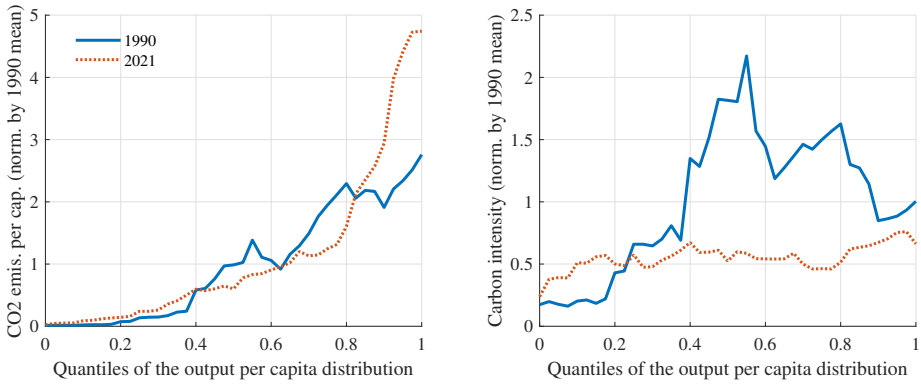

Notes. This figure shows how CO_2 emissions per capita and carbon intensity vary across the quantiles of the output per capita distribution in 1990 and 2021. Each series is smoothed using a moving average and normalized by the respective 1990 cross-sectional mean. Data sources are listed in Appendix A.

capacity and economic structures less exposed to climate-sensitive sectors, are less affected by temperature increases (see also Dell et al., 2012; Burke et al., 2015, for similar observations).

Taken together, these six regularities capture key features of the climate-economy system, including large cross-country differences and the alarming accumulation of atmospheric CO_2.

3. The Model

Following Golosov et al. (2014) and Hillebrand and Hillebrand (2019), we consider a multi-sector neoclassical growth model in which production may generate carbon emissions, depending on the type of energy used. These emissions accumulate in the atmosphere and reduce economic output. We depart from these papers along two key dimensions. First, we assume a continuous-time framework with a continuum of countries that only differ in their initial capital stock. Second, atmospheric CO_2 affects output growth, rather than the output level. These choices allow us to characterize the entire economy using a system of two partial differential equations and two ordinary differential equations, converging to an asymptotically stable steady state. Our assumptions are formalized below.

Assumption 1 (Initial heterogeneity across countries)**.** *There exists a continuum of countries that differ only in their initial capital stock.*

Assumption 2 (Atmospheric CO_2 and growth)**.** *The world economy grows at a rate $p(t)$, which is not constant but depends on atmospheric CO_2. The rate $p(t)$ is the sum of growth rate of labor input $n(t) \coloneqq \dot{N}(t)/N(t)$ and growth rate of labor-augmenting technological progress $g(t) \coloneqq \dot{A}(t)/A(t)$.*

Assumptions 1 and 2 imply that countries have different output *levels* but the same exogenous *growth* rate. This is consistent with Nath et al. (2024), who, using data from 1960

to 2019 from the Penn World Tables, show that level differences across countries persists, but that growth differences do not.

The second part of Assumption 2 – that atmospheric CO_2 affects productivity growth rather than productivity levels – is motivated both by empirical evidence and by tractability. Empirically, Chang et al. (2023) shows that level-effect specifications understate climate damages relative to models with growth effects, because temperature impacts accumulate over time. From a theoretical perspective, in the standard neoclassical growth model the long-run growth rate, driven by labor growth and technological progress, is constant, implying that non-detrended variables grow without bound. In our model, positive long-run growth would imply unbounded atmospheric CO_2 concentrations. Linking CO_2 negatively to productivity growth prevents this outcome.

Finally, under a continuous distribution, each country is atomistic and thus considers its emissions as having a negligible impact on global atmospheric CO_2 and output growth.

3.1. **Setup.** Each country consists of a representative household, a final goods producing sector, and two energy sectors producing either brown or green energy. Brown energy production generates carbon emissions because it relies on fossil fuels purchased on an international market. Emissions from all countries accumulate in the atmosphere, affecting global output growth. We detail these components in the following subsections. Unless otherwise specified, we present the model in detrended form. That is, any lowercase variable $z(t)$ denotes the detrended counterpart of its non-detrended form $Z(t)$, defined as $z(t) \coloneqq Z(t)/(A(t)N(t))$.

3.1.1. *Representative household.* In each country, there is a single representative household whose preferences are described by an additive utility function with a constant rate of time preference $\rho \geq 0$, given by

$$\int_0^\infty \mathrm{e}^{-\rho t} \, \frac{\big(A(t)\, N(t)\, c(t)\big)^{1-\sigma} - 1}{1-\sigma} \, \mathrm{d}t \,,$$

where $c(t)$ denotes detrended household consumption and $\sigma > 0$ is the inverse of the intertemporal elasticity of substitution (IES). We thus adopt the standard classical-utilitarian utility specification with discounting (see, for instance, Acemoglu, 2009). The detrended level of capital stock $k(t)$ evolves as

$$\dot{k}(t) = w(t) + \big(r(t) - (p(t) + \delta)\big)k(t) - c(t) \,,$$

where $w(t)$ is labor income, and detrended labor supply is exogenous and normalized to one. Variable $r(t)$ denotes the real return on capital. The growth rate $p(t)$ is the sum of the growth rates of labor and labor-augmenting technological progress (see Assumption 2), $\delta > 0$ is the capital depreciation rate, and $k_0 \geq 0$ is the initial capital endowment, which is given and varies across countries (see Assumption 1).

3.1.2. *Production sectors.* Each country has three production sectors: a final goods sector (subscript f), which produces final output $y(t)$ using capital, labor, brown energy, and green energy; a brown energy sector (subscript b), which produces brown energy $e_b(t)$ using capital, labor, and fossil fuels; and a green energy sector (subscript g), which produces green energy $e_g(t)$ using capital and labor.

Assumption 3 (Closed economies)**.** *There is no international trade in capital, labor or energy.*

This assumption is standard in the literature since the seminal Nordhaus multi-region integrated assessment RICE model and appears in Hassler and Krusell (2012), as well as many subsequent contributions. We discuss an extension with an international capital market in Section 8.

We now describe production in each sector. Let $\theta_i > 0$ denote the productivity level in sector $i \in \{f, b, g\}$, and let $k_i(t)$ and $n_i(t)$ denote the capital and labor inputs in that sector. We assume Cobb-Douglas production technologies in all sectors, with elasticities $\alpha_i \in (0, 1)$, $\mu_i \in (0, 1 - \alpha_i)$, and $\nu_i \in (0, 1 - \alpha_i - \mu_i)$.[7]

The production functions in the three sectors are

$$\begin{aligned} y(t) &= \theta_f k_f(t)^{\alpha_f}\, e_b(t)^{\mu_f}\, e_g(t)^{\nu_f}\, n_f(t)^{1-\alpha_f-\mu_f-\nu_f}\,, \\ e_b(t) &= \theta_b k_b(t)^{\alpha_b}\, x(t)^{\mu_b}\, n_b(t)^{1-\alpha_b-\mu_b}\,, \\ e_g(t) &= \theta_g k_g(t)^{\alpha_g}\, n_g(t)^{1-\alpha_g}\,. \end{aligned}$$

Since renewable resources (such as wind or sun) are freely available, they do not appear explicitly in the green energy production function. In contrast, brown energy production requires fossil fuels $x(t)$, which are purchased on an international market (see Section 3.1.3 for details).

Assumption 3 states that there is no international trade in capital and labor. As a result, the following market-clearing conditions hold

$$\begin{aligned} k(t) &= k_f(t) + k_b(t) + k_g(t)\,, \\ 1 &= n_f(t) + n_b(t) + n_g(t)\,, \end{aligned}$$

where the total labor supply is normalized to one.

[7]We assume the elasticity of substitution between brown and green energy is 1, as in Acemoglu et al. (2012) and Rezai and van der Ploeg (2015). This allows us to express final output as an explicit function of aggregate capital only. Section 8 considers a more general CES specification, as in Golosov et al. (2014) and Hillebrand and Hillebrand (2019).

3.1.3. *Fossil fuel extraction.* We denote world demand for fossil fuels by $\bar{x}(t)$ and we assume this aggregate demand is satisfied by a single representative country whose sole role is to extract and sell fossil fuels. The extractor faces a constant per-unit extraction sunk cost $c_x > 0$.

We further suppose that fossil fuel reserves are unlimited, so no supply-side constraints arise. While the total amount of fossil fuels is unknown, it is likely to be large, suggesting that reserves could support significant extraction for many decades (Hassler et al., 2016). We finally assume that the net trade balance between the fossil fuel extracting country and every other country is zero. The extractor exports fossil fuels and imports final goods to cover its extraction costs. We therefore impose that the value of energy exports to each country is exactly offset by the value of imports from that country.

3.1.4. *Climate determinants.* Carbon emissions arise from burning fossil fuels $x(t)$ during brown energy production at the level of each country. However, the accumulation of CO_2 in the atmosphere depends on aggregate use of fossil fuels $\bar{x}(t)$. Let $\epsilon > 0$ be the emissions coefficient converting fossil fuel use into atmospheric CO_2, and let $\psi > 0$ denote the natural decay rate of atmospheric CO_2. Atmospheric CO_2 $s(t)$ evolves as

$$\dot{s}(t) = \epsilon\, \bar{x}(t) - \big(\psi + p(t)\big) s(t)\,, \tag{1}$$

where $s_0 > 0$ is its initial value.

Atmospheric CO_2 lowers the growth rates of labor and labor-augmenting technological progress, summarized by $p(t)$ (see Assumption 2). Specifically, we assume

$$\dot{p}(t) = -\,\gamma\, \frac{\dot{S}(t)}{S(t)}\,, \tag{2}$$

where $S(t)$ denotes the *non-detrended* level of atmospheric CO_2. In words, increases in the non-detrended CO_2 stock reduce the rate of economic growth, with $\gamma \geq 0$ measuring the strength of this effect. After detrending and inserting equation (1), we have

$$\dot{p}(t) = -\,\gamma \left(\frac{\epsilon\, \bar{x}(t)}{s(t)} - \psi \right),$$

with the initial growth rate p_0 given.

3.2. **Equilibrium conditions and asymptotic stability.** This section derives the equilibrium conditions. All agents behave optimally under perfect foresight, and all markets are perfectly competitive. Given the continuous distribution of countries, each country is atomistic and therefore takes $p(t)$ as given.

3.2.1. *Equilibrium conditions.* To simplify the exposition, we aggregate several parameters.

Definition 1 (Aggregate parameters)**.** *We first combine the different elasticity and productivity parameters as*

$$\begin{aligned}
\mu &\coloneqq 1 - \mu_f \mu_b \in (0,1)\,, \\
\alpha &\coloneqq \alpha_f + \mu_f \alpha_b + \nu_f \alpha_g \in (0,1)\,, \\
\tilde{\theta} &\coloneqq \theta_f\, \theta_b^{\mu_f}\, \theta_g^{\nu_f} > 0\,.
\end{aligned}$$

We then define the function $\Lambda(z_1, z_2, ..., z_n) \coloneqq \prod_{i=1}^{n} \omega_i^{z_i}$*, with* $\omega_i \coloneqq \frac{z_i}{\sum_{i=1}^{n} z_i}$*, for* $z_i \in (0,1)$ *and* $\sum_{i=1}^{n} z_i \in (0,1)$*, which allows us to write*

$$\begin{aligned}
\tilde{k} &\coloneqq \Lambda(\alpha_f, \mu_f \alpha_b, \nu_f \alpha_g) > 0\,, \\
\tilde{n} &\coloneqq \Lambda\left(1 - \alpha_f - \mu_f - \nu_f, \mu_f(1 - \alpha_b - \mu_b), \nu_f(1 - \alpha_g)\right) > 0\,.
\end{aligned}$$

Finally, we define

$$\begin{aligned}
\phi &\coloneqq \epsilon\, \frac{\mu_f \mu_b}{c_x} > 0\,, \\
\tilde{x} &\coloneqq \left(\frac{\mu_f \mu_b}{c_x}\right)^{\mu_f \mu_b} > 0\,, \\
\tilde{y} &\coloneqq \left(\tilde{\theta}\, \tilde{k}\, \tilde{n}\, \tilde{x}\right)^{\frac{1}{\mu}} > 0\,.
\end{aligned}$$

The first set of aggregate parameters $\{\mu, \alpha, \tilde{\theta}\}$ is relatively intuitive to interpret. By embedding the production functions of brown and green energy into the final goods production function, we obtain an 'aggregate' final goods production function (see Appendix B for details). In this aggregate specification, μ represents the share of all inputs other than fossil fuel, and α is the share of all capital inputs. The ratio $\alpha/\mu \in (0,1)$ thus captures the net capital share; that is, the capital share in production excluding fossil fuel. Similarly, $(\mu - \alpha)/\mu \in (0,1)$ represents the net labor share. Lastly, $\tilde{\theta}$ corresponds to aggregate total factor productivity.

The second set of parameters, $\tilde{k}$ and $\tilde{n}$, serve as aggregate scaling parameters for capital and labor. They are based on the function $\Lambda(\cdot)$, which aggregates the shares of each type of capital and labor used in final goods production. Since we consider three types of capital and three types of labor, the function Λ takes three arguments for each case.

The third set of parameters relates to fossil fuels: ϕ converts final goods output into atmospheric CO_2, while $\tilde{x}$ is a scaling parameter for fossil fuel use. Both ϕ and $\tilde{x}$ increase with the ratio $(\mu_f \mu_b)/c_x$, which captures the share of fossil fuel use in production relative to the

extraction cost. Finally, $\tilde{y}$ combines the aggregate total factor productivity and the scaling parameters for capital, labor, and fossil fuels.

With these definitions in place, the following proposition presents the equilibrium conditions.

Proposition 1 (Equilibrium conditions with heterogeneous countries)**.** *A competitive equilibrium consists of specific paths* $[c_j(t), k_j(t)]_{t=0}^{\infty}$ *for each country* j *and aggregate paths for atmospheric* CO_2 *and growth* $[s(t), p(t)]_{t=0}^{\infty}$ *satisfying the system*

$$\begin{cases} \dot{k}_j(t) &= \mu\, \tilde{y}\, k_j(t)^{\frac{\alpha}{\mu}} - (p(t)+\delta)k_j(t) - c_j(t)\,, \\ \frac{\dot{c}_j(t)}{c_j(t)} &= \frac{\alpha\, \tilde{y}\, k_j(t)^{\frac{\alpha}{\mu}-1} - (\rho+\delta)}{\sigma} - p(t)\,, \\ \dot{s}(t) &= \phi \int_j \tilde{y}\, k_j^{\frac{\alpha}{\mu}}\, \mathrm{d}j - (p(t)+\psi)s(t)\,, \\ \dot{p}(t) &= -\gamma \left(\frac{\phi \int_j \tilde{y}\, k_j^{\frac{\alpha}{\mu}}\, \mathrm{d}j}{s(t)} - \psi \right), \end{cases}$$

with initial capital stock $k_{j,0}$ *specific to each country* j*, as well as a transversality condition* $\lim_{t\to\infty} \mathrm{e}^{-\left(\rho t - (1-\sigma)\int_0^t p(u)\mathrm{d}u\right)} c_j(t)^{-\sigma} k_j(t) = 0$*. The initial values* s_0 *and* p_0 *are given. We also assume that initial labor and labor-augmenting technological progress are normalized to 1.*

Proof. See Appendix B. □

The first two differential equations correspond to the equilibrium conditions in the standard neoclassical growth model, with two departures. First, agents (here countries) are heterogeneous, differing in their initial capital stock $k_{j,0}$ (Assumption 1) and therefore following individual capital and consumption paths. Second, aggregate growth rate $p(t)$ is endogenous and reacts to atmospheric CO_2 $s(t)$. The last two differential equations capture the evolution of $s(t)$ and its impact on $p(t)$. Variable $s(t)$ depends on global production and the role of fossil fuels, as summarized by the parameter ϕ. In turn, higher atmospheric CO_2 lowers economic growth via its negative effect on $p(t)$, governed by the parameter γ.

We now turn to the asymptotic properties of the equilibrium.

3.2.2. *Asymptotic equilibrium.* The following proposition characterizes the interior steady state and establishes its existence.[8]

[8]We do not consider the corner steady state with no production and no consumption. Moreover, when $\sigma \geq 1$, utility would be undefined in this case.

Proposition 2 (Steady state)**.** *The equilibrium conditions in Proposition 1 admit a unique interior steady state given by*

$$\begin{cases} k^* &= \left(\frac{\alpha\,\tilde{y}}{\rho+\delta}\right)^{\frac{\mu}{\mu-\alpha}} \\ c^* &= \left(\frac{\mu\,(\rho+\delta)}{\alpha} - \delta\right) k^* \\ s^* &= \frac{\phi\,(\rho+\delta)}{\alpha\,\psi}\,k^* \\ p^* &= 0. \end{cases}$$

Proof. In steady state, $\dot{k}_j(t) = \dot{c}_j(t) = \dot{s}_j(t) = \dot{p}(t) = 0$. From the second equation in Proposition 1, we see that $k_j^* = k^*$ (all countries have the same capital at the steady state), and from the first equation that $c_j^* = c^*$. Then, combining the last two equations gives $p^* = 0$ (zero growth at the steady state). Finally, we immediately obtain the expressions for k^*, c^* and s^* from the first three equations. □

Appendix B shows that the determinant of the Jacobian matrix at the interior steady state is negative. This implies either (i) three negative and one positive eigenvalues, or (ii) one negative and three positive eigenvalues. In case (i), the steady state is asymptotically stable since the system has three state variables $\{k(t), s(t), p(t)\}$ and one control variable $c(t)$. In case (ii), there are too many unstable eigenvalues and the steady state is unstable. Although we cannot provide a general analytical proof of case (i), numerical computations based on our calibration yield the stable configuration. We therefore assume that the model admits a single asymptotically stable interior steady state.[9] Moreover, the steady state is independent of the initial capital stock k_0, meaning that all countries converge to the same long-run outcome despite differing initial conditions.

We also observe that $p^* = 0$ at the interior steady state, implying that non-detrended variables also reach a steady state. This feature is essential, for the – non-detrended – level of atmospheric CO_2 to stabilize rather than grow indefinitely. Moreover, Proposition 2 yields

$$s^* = \frac{\phi}{\psi}\,\tilde{y}^{\frac{\mu}{\mu-\alpha}}\,\left(\frac{\alpha}{\rho+\delta}\right)^{\frac{\alpha}{\mu-\alpha}}.$$

Hence, s^* increases with ϵ (the fossil-fuel-to-CO_2 conversion coefficient, which enters via ϕ), and decreases with ψ (the natural decay rate of atmospheric CO_2) and c_x (the fossil fuel extraction cost, which enters both ϕ and $\tilde{y}$). These comparative statics are intuitive: higher emissions per unit of fuel raise s^*, as does slower natural decay or lower extraction costs. Furthermore, s^* decreases with the rate of time preference ρ: a higher ρ induces households to value current consumption more, leading to lower investment, reduced long-run output, and hence lower steady-state emissions.

[9] Appendix B provides the analytical proof that the Solow-type version of the model, in which the saving rate is constant rather than endogenous, has three negative eigenvalues and is therefore stable.

3.3. **Mean field game system.** Proposition 1 characterizes the equilibrium for an individual country j but not for the world economy, as it does not consider the evolution of the cross-sectional distribution. To do so, we follow Achdou et al. (2022) and recast our model with heterogeneous agents into a system of partial differential equations, specifically a mean field game (MFG) system combining a backward Hamilton-Jacobi-Bellman equation and a forward transport equation. The next proposition fully describes the dynamic equilibrium of our model.

Proposition 3 (Backward–forward MFG system)**.** *The competitive equilibrium with heterogeneous countries presented in Proposition 1 can be characterized by a system of two partial differential equations (PDEs) and two ordinary differential equations (ODEs). The first PDE is a backward* ***Hamilton–Jacobi–Bellman (HJB) equation***

$$\rho\, v(t,k) \;=\; \max_{c} \left\{ \mathrm{e}^{(1-\sigma)\int_0^t p(u)\mathrm{d}u}\, \frac{c^{1-\sigma}}{1-\sigma} - \frac{1}{1-\sigma} + \frac{\partial v}{\partial k}(t,k)\left(\mu\,\tilde{y}\,k^{\frac{\alpha}{\mu}} - (p(t)+\delta)\;k - c\right) + \frac{\partial v}{\partial t}(t,k)\right\}, \tag{3}$$

where $(t,k) \in \mathbb{R}^+ \times \mathbb{R}^+$*. We impose Cauchy boundary conditions*

$$v(t,0) = -\,\frac{1}{\rho(1-\sigma)}\,,\ \text{for } \sigma \in (0,1)\,, \quad v(t,0) = -\infty\,,\ \text{for } \sigma \geq 1\,, \quad \frac{\partial v}{\partial k}(t,0) = +\infty\,,$$

and terminal condition

$$\lim_{t\to+\infty} k\,\frac{\partial v}{\partial k}(t,k)\,e^{-\rho t} = 0\,.$$

The second PDE is a forward ***transport equation***

$$\frac{\partial u}{\partial t}(t,k) = -\,\frac{\partial}{\partial k}\left(i(t,k)\,u(t,k)\right)\,, \tag{4}$$

where $i(t,k) \coloneqq \mu\,\tilde{y}\,k^{\frac{\alpha}{\mu}} - (p(t)+\delta)\,k - \left(\frac{\partial v}{\partial k}(t,k)\right)^{-\frac{1}{\sigma}} \mathrm{e}^{\frac{1-\sigma}{\sigma}\int_0^t p(u)\mathrm{d}u}$*, with Dirichlet boundary conditions*

$$u(t,0) = 0\,, \quad u(t,\infty) = 0\,,$$

and initial condition

$$u(0,k) = u_0(k) \geq 0\,,\ \textit{with} \int_0^\infty u_0(k)\,\mathrm{d}k = 1\,.$$

Finally, the ODEs are the ***climate equations***

$$\begin{cases} \dot{s}(t) &=& \phi\,\bar{k}(t) - (p(t)+\psi)s(t)\,, \\ \dot{p}(t) &=& -\,\gamma\left(\frac{\phi\,\bar{k}(t)}{s(t)} - \psi\right)\,, \end{cases} \tag{5}$$

where $\bar{k}(t) \coloneqq \int_0^\infty \tilde{y}\,k^{\frac{\alpha}{\mu}} u(t,k)\,\mathrm{d}k$*, and with initial conditions*

$$s(0) = s_0 \geq 0\,, \quad p(0) = p_0\,.$$

Proof. See Appendix C. □

The HJB equation describes the optimal choices of atomistic countries for any level of capital k and time t. This equation takes as given the distribution of all other countries, summarized by the aggregate productivity variable $p(t)$. Solving the HJB equation amounts to finding the function $v(t, k)$, known as the value function, which represents the discounted sum of all future utility for a country with capital stock k at time t. The boundary conditions arise directly from the utility function, and the terminal condition is the standard transversality condition that rules out explosive solutions in infinite-horizon problems.

The transport equation, also known as the unidirectional wave equation, tracks the distribution of countries, taking the optimal choices from the HJB equation as given. Solving the transport equation amounts to finding the function $u(t, k)$, which represents the density of countries with capital k at time t. The initial distribution is normalized so that total density equals one. Because the transport equation is written in conservative form, total density is preserved over time. When $i(t, k) < 0$, the density shifts leftward, and when $\frac{\partial i(t,k)}{\partial k} < 0$, the density compresses around lower capital values (see Garcia and Pierrard, 2025, for a similar discussion). For a detailed introduction to the transport equation, see Olver (2014). In our MFG system, this equation has two companion equations – the climate equations – which use the evolving distribution to compute the aggregate level of carbon concentration and its effect on aggregate productivity.

The HJB and transport equations are coupled: the HJB requires the distribution from the transport equation (through $p(t)$), and the transport equation needs the optimal choices from the HJB (through $i(t, k)$). Moreover, the HJB equation runs backward, meaning it takes future values into account to determine current choices; while the transport equation runs forward, computing the distribution at time $t + \mathrm{d}t$ from the distribution and optimal choices at t. Combined, the HJB and transport equations therefore form a backward–forward MFG system.

4. Computation

We now describe our algorithm for solving the backward-forward MFG system in Proposition 3. Readers not concerned with numerical computation may skip this section.

4.1. **Bird's eye view of algorithm.**

Our goal is to solve the MFG system on the rectangle $[t_\ell, t_h] \times [k_\ell, k_h]$ for a given initial distribution of capital $u(t_\ell, \cdot)$, atmospheric CO_2, $s(t_\ell)$, and growth rate $p(t_\ell)$. Taking $t_h \to \infty$ gives the full transition path to the interior steady state in Proposition 2.

As mentioned before, the key difficulty is that the four differential equations in the MFG system are coupled. Each country chooses savings and consumption while anticipating future

losses from atmospheric CO_2. These losses depend on global emissions. Hence, each country must consider the production, consumption, and investment of its peers. The capital distribution $u(t,k)$ therefore enters each country's policy function. This obstacle is standard in heterogeneous agent models, whether posed in discrete time (e.g., Krusell and Smith, 1998) or continuous time (e.g., Achdou et al., 2022).

To address this issue, we follow Den Haan (1997) and Krusell and Smith (1998) and used a fixed-point algorithm. We assume that the law of motion for $p(t)$ is

$$p(t) = f(t|\mathbf{\Theta}), \tag{6}$$

where $f(t)$ is an analytic function parametrized by a vector $\mathbf{\Theta}$.

Crucially, for a given vector $\mathbf{\Theta}$, the HJB equation governing consumption-saving choices is independent of the other three differential equations in the MFG system, suggesting a simple iterative procedure. Starting from an initial guess $\mathbf{\Theta}_0$, for $i = 0, 1, 2, ...$ we perform

(1) Given $\mathbf{\Theta}_i$, solve the HJB equation (3) and compute $i(t,k)$.
(2) Solve the transport equation (4) and compute $\bar{k}(t)$.
(3) Solve the system of ODEs (5).
(4) Use the resulting time path $\{p(t)\}_{t=t_\ell}^{t_h}$ to estimate $\mathbf{\Theta}_{i+1}$.

We iterate until the parameter vector $\mathbf{\Theta}$ converges, then verify that the fit is satisfactory. As the overall algorithm is standard (see, e.g., Heer and Maußner, 2024, for a textbook treatment on solving heterogeneous agent models), the remainder of this section focuses on the aspects specific to our model: solving the two nonlinear partial differential equations (3) and (4).

4.2. **Solving the HJB equation.** We need to approximate the unknown value function $v(t,k) \in \mathbb{R}^+ \times \mathbb{R}^+ \to \mathbb{R}$ on the rectangle $[t_\ell, t_h] \times [k_\ell, k_h]$, given the perceived law of motion for $p(t)$ in equation (6). The function $v(t,k)$ satisfies the functional HJB equation (3), written in operator form as

$$\mathcal{H}[v(t,k)] = 0.$$

Let $T >> t_h$ be a large integer such that $e^{-\rho(T-t_h)} \approx 0$. Given the perceived law of motion for $p(t)$, the first two ODEs in Proposition 1 describe the optimal paths of capital and consumption on $[t,T]$, for a given initial capital $k(t)$ and terminal consumption equal to the steady-state level c^*. This defines a nonlinear boundary value problem (BVP) that can be solved using standard numerical methods. With the optimal paths, the value function can be approximated by numerically integrating the discounted future utility flows.

More precisely, we approximate $v(t,k)$ on $[t_\ell, t_h] \times [k_\ell, k_h]$ as follows.

(1) Construct a two-dimensional grid of points (t_i, k_j) on $[t_\ell, t_h] \times [k_\ell, k_h]$.

(2) At each grid point (t_i, k_j), use the collocation method proposed by Shampine et al. (2003) to solve the nonlinear BVP defined by the first two ODEs in Proposition 1, with boundary conditions $k(t_i) = k_j$ and $c(T) = c^*$, with $T >> t_h$. This yields the optimal paths of capital and consumption on $[t_i, T]$.

(3) Approximate the value function at each grid point as the discounted sum of future utility flows

$$\hat{v}(t_i, k_j) = \int_{t_i}^{T} e^{-\rho(s-t_i)} \frac{\left(A(s)N(s)c^{**}(s)\right)^{1-\sigma} - 1}{1-\sigma} \, \mathrm{d}s,$$

where $c^{**}(s)$ is the optimal consumption path obtained in step 2.

We assess accuracy by computing the residual $R(t,k) = \mathcal{H}[\hat{v}(t,k)]$ on a finer grid within the same domain. The function $\hat{v}$ is evaluated on this finer grid using cubic interpolation. This procedure tests the approximation beyond the original grid points, capturing both interpolation and discretization errors. As shown in Appendix D, the residual remains close to zero across the entire rectangle.

This indirect approach to solve the HJB functional equation offers several numerical advantages compared to alternatives, such as projection methods (see e.g., Fernandez-Villaverde et al., 2016) or finite-difference methods (see e.g., Achdou et al., 2022). In particular, working with a system of ODEs tends to be less demanding than solving a PDE. For example, we can impose that consumption converges to its steady-state value at time T, which is simpler than imposing the equivalent terminal condition on the value function. It is also easier to generate good initial guesses and to apply homotopy methods. Moreover, trial and error shows that the indirect approach is both faster and more stable in our setup.

4.3. **Solving the transport equation.** With the HJB equation solved and the countries' policy functions in hand, we are ready to tackle the transport equation (4). Since the latter is a fundamental partial differential equation in physics, where it is widely used to model first-order wave dynamics, we draw on the extensive literature on finite difference methods for its numerical solution. Broadly, we replace the derivatives in the transport equation with numerical differentiation formulas.

Since $i(t,k)$ may take both positive and negative values, we use a standard upwind scheme: a forward difference approximation for $\frac{\partial}{\partial k}u(t,k)$ when $i(t,k) < 0$, and a backward difference when $i(t,k) > 0$. We verify that the Courant–Friedrichs–Lewy condition holds at every node

in $[t_\ell, t_h] \times [k_\ell, k_h]$, providing numerical stability in all our computations.[10] For a detailed discussion of finite difference schemes for wave models, see Chapter 5 of Olver (2014).

4.4. **Summary.** Overall, the algorithm delivers solutions that are accurate and robust. Extensive checks are reported in Appendix D.

5. Mapping the Model to the Data

In this section, we first calibrate our parameters to reproduce selected targets. We then evaluate how well this calibrated model reproduces the five empirical regularities described in Section 2.

5.1. **Calibration.** We assign parameter values to match key features (targets) of the world economy in 1990-2021. Because our model links the climate and the economy, most parameters have units. For instance, the model converts fossil fuels (expressed in tons) into energy (in watt-hours), and then into production (in 2011 U.S. dollars), while generating CO_2 emissions (in tons). Table 2 summarizes the calibration – including units and the target associated with each parameter – and we defer all other details and references to Appendices A.1 and A.2. We highlight several important features below.

5.1.1. *Time period.* Since the model is designed to reproduce key developments in the world economy and climate between 1990 and 2021, we impose $t = 0$ for 1990 and $t = 1$ for 2021. One model period thus corresponds to 32 years ($\Delta t = 32$ years).

5.1.2. *Normalizations.* In each country, we normalize the initial labor-augmenting technological progress and labor force to 1 ($A(0) = N(0) = 1$; see Proposition 1). In January 1990, atmospheric CO_2 concentration at the Mauna Loa Observatory was 356 parts per million (National Oceanic and Atmospheric Administration), equivalent to 2,760 gigatons (Gt) of CO_2. We normalize this initial concentration to one, $s_0 = 1$, which implies a normalization constant of $n = 2{,}760$. This normalization also affects other parameters (see the 'Unit' column in Table 2). Finally, because the model is expressed in real terms, all prices are expressed in 2011 U.S. dollars.

5.1.3. *Distribution of countries.* Assumption 1 requires that countries differ in their initial capital stocks k_0, with $u(0, k) = u_0(k)$ denoting the initial probability density function. We construct the empirical counterpart of $u_0(k)$ using the Penn World Table (Feenstra et al., 2015) for a sample of 134 countries. According to the World Bank, 50 of these countries are classified as high-income. Several of our calibration targets should be GDP-weighted averages across countries (e.g. the average share of green energy or the average carbon intensity in

[10] Although the HJB and transport equations are solved on the same rectangle $[t_\ell, t_h] \times [k_\ell, k_h]$, the transport equation requires a much finer grid. We therefore use cubic interpolation to evaluate the policy function $i(t, k)$ on this finer grid.

1990). However, data are not always available for the full set of 134 countries. Therefore, instead of targeting the weighted average across the full sample, we often target the median across the 50 high-income countries, for which data availability is more consistent.

5.1.4. *Elasticities of output with respect to energy.* Between 1990 and 2021, the cross-country median share of alternative and nuclear energy in total energy use increased by a factor of 2.6 across 134 countries and by a factor of 1.9 across the subset of 50 high-income countries. To capture this trend, we assume green energy-biased technological progress (see, for example, Zhao et al., 2026, for empirical evidence). That is, we let the elasticity of final output with respect to brown energy, μ_f, decrease over time, while the elasticity with respect to green energy, ν_f, increases over time, according to the logistic functions

$$\mu_f(t) = \frac{\mu_{f0} + \nu_{f0}}{1 + \frac{\nu_{f0}}{\mu_{f0}} \mathrm{e}^{\kappa t}}, \qquad \nu_f(t) = \frac{\mu_{f0} + \nu_{f0}}{1 + \frac{\mu_{f0}}{\nu_{f0}} \mathrm{e}^{-\kappa t}},$$

with μ_{f0} and ν_{f0} in $[0, 1)$, and $\kappa > 0$. These functions satisfy $\mu_f(0) = \mu_{f0}$, $\nu_f(0) = \nu_{f0}$, and $\mu_f(t) + \nu_f(t) = \mu_{f0} + \nu_{f0}$, implying that although each elasticity varies over time, their sum is constant. Moreover, $\mu_f(t) \to 0$ as $t \to \infty$, meaning that brown energy is eventually phased out, and thus $\nu_f(t) \to \mu_{f0} + \nu_{f0}$.

5.1.5. *Total factor productivity of the final firms.* As noted above, we consider a single source of heterogeneity (the initial distribution of capital; see Assumption 1), and all economies converge to the same asymptotic steady state (Proposition 2). In the absence of additional mechanisms that sustain cross-country differences, heterogeneity dissipates quickly: after one time unit (32 years), all countries become virtually identical. This is not consistent with the data, which exhibit persistent cross-country disparities.[11] To preserve a meaningful cross-sectional distribution, we follow Krueger et al. (2016) and introduce an aggregate-demand externality. Specifically, we assume that total factor productivity in the final-goods sector is partly demand-driven (for microfoundations see Kaplan and Menzio, 2016; Bai et al., 2025). As a result, firms in richer countries – which have higher capital stocks and thus higher demand – benefit from a positive externality on productivity, allowing these countries to remain richer for longer. The opposite holds for firms in poorer countries.[12] More precisely, we assume that total factor productivity in sector f is no longer the constant θ_f, but the function $\theta_f(t, k) > 0$ satisfying: $\theta_f(t, k_{0,\mu}) = \theta_{f0}$, $\lim_{t\to\infty} \theta_f(t, k) = \theta_{f0}$, and $\partial\theta_f(t, k)/\partial k > 0$, where $k_{0,\mu}$ is the mean initial capital stock. Thus, in the average country, productivity equals θ_{f0}; in the long run productivity converges to θ_{f0} for all countries; and productivity increases

[11] This strong convergence is a generic property of the neoclassical growth model.

[12] An alternative mechanism, as in De Nardi et al. (2024), would be to assume that rich countries are more patient. While both approaches imply similar qualitative dynamics, making TFP demand-driven allows us to more closely match the data.

with capital. The function

$$\theta_f(t,k) = \theta_{f0}\left(1 + \mathrm{e}^{-\beta_g t}\,\frac{1-\mathrm{e}^{-\beta_f(k-k_{0,\mu})}}{1+\mathrm{e}^{-\beta_f(k-k_{0,\mu})}}\right),$$

with $\beta_f > 0$ and $\beta_g > 0$, satisfies these requirements. The parameters β_f and β_g govern the speed of adjustment (or steepness) with respect to k and t.

5.1.6. *Growth rates.* Our model does not distinguish between the labor growth rate $n(t)$ and the labor-augmenting technological progress growth rate $g(t)$. Only their sum, $p(t)$, appears in the equations and is affected by atmospheric CO_2 (Proposition 3). However, many results are presented in per-capita terms, which requires specifying how CO_2 affects each component of growth. Empirical evidence suggests that climate change impacts both types of growth. For instance, in the United States, one additional day of extreme heat increases the annual mortality rate by 0.11% (Deschênes and Greenstone, 2011). This effect is larger in developing countries (Geruso and Spears, 2018). Moreover, environmental conditions affect labor productivity too (Graff Zivin and Neidell, 2012; OECD, 2016). As a result, we assume that atmospheric CO_2 affects labor growth and labor-augmenting technological progress symmetrically. That is, total growth is split according to $n(t) = \lambda p(t)$ and $g(t) = (1-\lambda)p(t)$, with $\lambda = 0.5$ (see Table 2).

5.1.7. *Other remarks.* First, the logistic functions $\mu_f(t)$ and $\nu_f(t)$ depend only on t, and their sum is constant. Although $\theta_f(t,k)$ depends on k, we treat it as an externality, and all θ_f values converge to a unique long-run value. As a result, Proposition 1 (equilibrium conditions), Proposition 2 (steady state), and Proposition 3 (MFG system) remain valid. Second, there is not always a direct one-to-one relationship between parameter values and calibration targets. For example, to calibrate $\{\kappa, \theta_{f0}, \beta_f, \beta_g\}$, we construct a coarse grid for these four parameters and evaluate the model at each grid point. For each parameter combination, we compare the model's implications with four empirical targets and select the combination that minimizes the distance to the data.[13]

5.2. **Validation.** We now study how well the model matches the six empirical regularities presented in Section 2. At the exception of the evolution of atmospheric CO_2, none of these empirical regularities were used as targets in the calibration procedure. As a stepping stone, we first assess how well the model replicates cross-sectional distributions in 1990, our initial year, of the three variables that form the identity

$$\text{Carbon intensity} = \frac{\text{CO}_2 \text{ emissions per capita}}{\text{Output per capita}},$$

which underpins our empirical regularities. Solid blue lines in Figure 3 show the estimated probability density functions for output and emissions per capita, across our sample of 134

[13]Full estimation is not feasible because solving the MFG system is numerically demanding.

TABLE 2. Parameter values

Parameter	Description	Unit	Value	Target
Representative household				
ρ	Discount rate	$1/\Delta t$	0.30	1% annual real interest rate
σ	Inverse IES	None	1.00	Literature, standard value
δ	Depreciation rate	$1/\Delta t$	1.98	6% annual capital depreciation rate
λ	Share growth labor	None	0.50	Literature, see text
Initial conditions (1990)				
s_0	Atmospheric CO_2	n Gt	1.00	Normalization
p_0	Growth rate	$1/\Delta t$	1.26	4% annual growth techno. + labor
$A(0)$	Technology level	None	1.00	Normalization
$N(0)$	Labor level	None	1.00	Normalization
$u_0(k)$	Distribution of k	None	$\mathcal{K}(\cdot)$	Capital to output distribution across 134 countries
Climate determinants				
c_x	Extraction cost	$\frac{n\ \$}{\text{t f. fuel}}$	0.07	\$28/barrel Brent crude oil in 1990
ϵ	Emission factor	$\frac{n\ \text{t } CO_2}{\text{kt f. fuel}}$	1.08	1 ton of fossil fuel emits 3 tons of CO_2
ψ	Decay rate	$1/\Delta t$	0.17	75% of 1 unit CO_2 absorbed after 300 years
γ	Damage parameter	$1/\Delta t$	0.42	1°C of warming reduces annual growth by 0.5 ppt
Production sectors				
μ_{f0}	Elasticity y_0 wrt e_{b0}	None	0.04	4% output share of brown exp. (1990, med. rich)
ν_{f0}	Elasticity y_0 wrt e_{g0}	None	0.02	2% output share of green exp. (1990, med. rich)
κ	Steepness μ_f	None	0.80	10% total energy is green (2021, med. rich)
α_f	Elasticity y wrt k_f	None	0.38	56% labour share income (1990-2021, med. rich)
μ_b	Elasticity e_b wrt x	None	0.78	0.45 (kg CO_2/\$) carbon intensity (1990, med. rich)
α_g	Elasticity e_g wrt k_g	None	0.75	Literature, Hillebrand and Hillebrand (2019, 2023)
α_b	Elasticity e_b wrt k_b	None	0.13	1.5% total empl. in energy sectors (1990, med. rich)
θ_b	TFP brown energy	Text	3.7e7	5.2% total energy is green (1990, med. rich)
θ_g	TFP green energy	Text	5.5e7	2.03 (kWh/\$) energy/output (1990, med. rich)
θ_{f0}	TFP final goods	Text	0.73	18% rise in atm. CO2 (1990 to 2021)
β_f	Steepness wrt k	None	15.0	130% rise in median capital p.c. (1990 to 2021)
β_g	Steepness wrt t	None	0.20	30% fall in CV capital p.c. (1990 to 2021)

Notes. One time unit represents 32 years (i.e., $\Delta t = 32$), $n = 2,760$ is a normalization constant, and all values expressed in USD dollars are in constant 2011 price. We use the following abbreviations: t for ton, g for gram, Wh for watt-hour, k for kilo (10^3) and G for giga (10^9). Moreover 'f. fuel' means fossil fuel, 'med. rich' the median of high-income countries, 'p.c.' per capita and 'CV' coefficient of variation. We fit the distribution $u_0(k)$ with an Epanechnikov kernel distribution $\mathcal{K}(\cdot)$. The resulting mean is $k_{0,\mu} = 0.07$. Finally, 'Text' means we provide more details in Section 5.1 and/or Appendix A.2; and the link between atmospheric CO_2 and warming is from Matthews et al. (2009, 2012) and detailed in footnote 14.

economies, while red dotted lines display the model counterparts. Each variable is normalized by its mean to make it unitless. The model places the mode close to the mode in the data, captures the observed dispersion, and reproduces the long right tail. For carbon intensity,

FIGURE 3. Comparison of 1990 cross-sectional densities

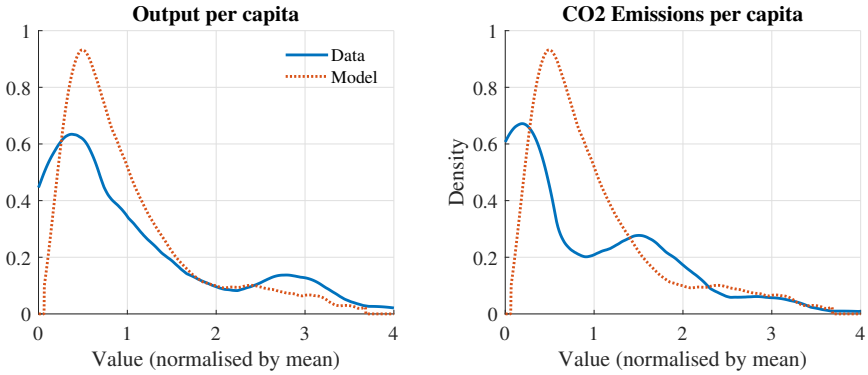

Notes. The figure compares the cross-sectional densities of output per capita and CO_2 emissions per capita in 1990. To make the variables unitless, each series is normalized by its corresponding mean. The densities from the data, which include 134 countries, are estimated with an Epanechnikov kernel.

the model implies (see Appendix B.4 for details)

$$\text{Carbon intensity} = \frac{\epsilon\, x(t)}{y(t)} = \frac{\epsilon\, \mu_f(t)\mu_b}{c_x}\,.$$

Carbon intensity does not depend on k, and is therefore identical across countries. This produces a degenerate distribution, so the model cannot capture the dispersion or the right tail of the observed 1990 distribution (see Table 1 in Section 2). That said, because cross-sectional dispersion in carbon intensity has collapsed between 1990 and 2021, the degenerate assumption becomes increasingly realistic over time. Overall, the model provides a good representation of the world economy's initial conditions. We now turn to how well it matches our six empirical regularities.

5.2.1. *Empirical regularities 1, 2 and 3.* Table 3 compares changes in the median and standard deviation of our three key variables in the data and in the model between 1990 and 2021. The model reproduces the large rise in output per capita, the much milder increase in CO_2 emissions per capita, and the decline in carbon intensity. Because all countries in our model converge deterministically to the same steady state, the model fails to match the sharp increase in the standard deviation of output per capita observed in the data. In addition, it slightly overstates the change in the standard deviation of emissions per capita, while matching its negative sign. As for carbon intensity, the data display the strong decline in dispersion discussed earlier, bringing the model closer to the data over time.

5.2.2. *Empirical regularity 4.* Moving to the link between output, emissions, and carbon intensity, Figure 4 shows CO_2 emissions per capita and carbon intensity in 2021, normalized by their 1990 means, across the output-per-capita distribution. The model captures the increasing, convex relationship between output and emissions, although it predicts a slightly flatter gradient than in the data. As already discussed above, for carbon intensity, the

TABLE 3. Evolutions (in %) between 1990-2021 of cross-sectional densities

	Output pc		*CO_2 emissions pc*		*Carbon intensity*	
	Data	Model	Data	Model	Data	Model
Median	+114	+70	+19	+19	-37	-29
Stand. Dev.	+126	+4	-3	-27	-77	–

Notes. The table reports the percent change between 1990 and 2021 for the median and the standard deviation of the distributions, both in the data (134 countries) and in the model. Since carbon intensity has a degenerate distribution in our model, the evolution of its standard deviation is irrelevant.

FIGURE 4. Emissions and carbon intensity across the output distribution in 2021

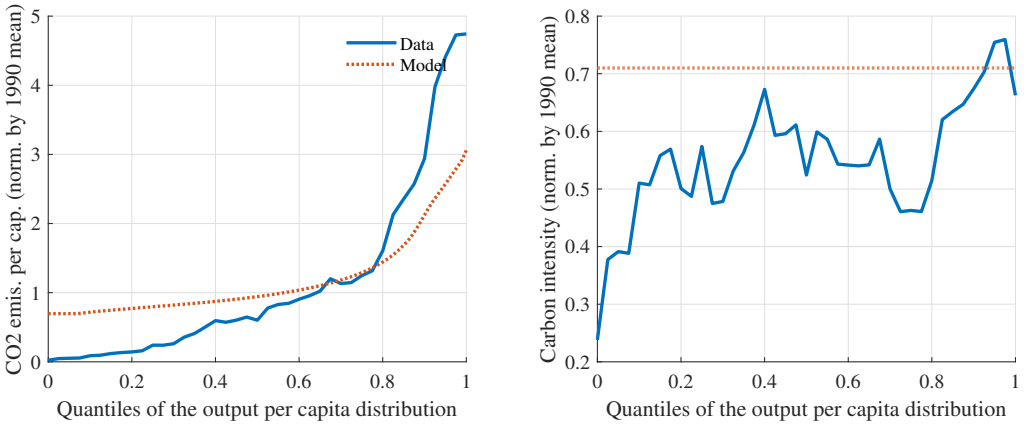

Notes. The solid lines show the empirical relationship between the quantiles of the output per capita distribution and CO_2 emissions (left panel) and energy use (right panel), based on data for 134 countries. The data is smoothed using a moving average and normalized by 1990 means. The dotted lines show the corresponding model-implied relationships.

model's degenerate distribution generates a flat profile across output per capita, which is consistent with the pattern observed in 2021.

5.2.3. *Empirical regularity 5.* The model generates a 23% increase in atmospheric CO_2 between 1990 and 2021, slightly above the 18% observed in the data. As noted in Section 5.1 and Appendix A.2, the 2021 atmospheric CO_2 was a target in the grid search used to calibrate a subset of parameters. The model does not match the target exactly, because the computational burden of solving the model requires using a coarse grid.

5.2.4. *Empirical regularity 6.* We finally examine the long-term economic costs of higher atmospheric CO_2 across the output distribution. To do so, we compare the output distribution from 2021 to 2100 in our baseline model with a version where CO_2 does not affect the growth rates of labor and labor-augmenting technology (i.e., $\gamma \to 0$). Output losses at quantile q at

FIGURE 5. Output losses per degree Celsius across the output distribution

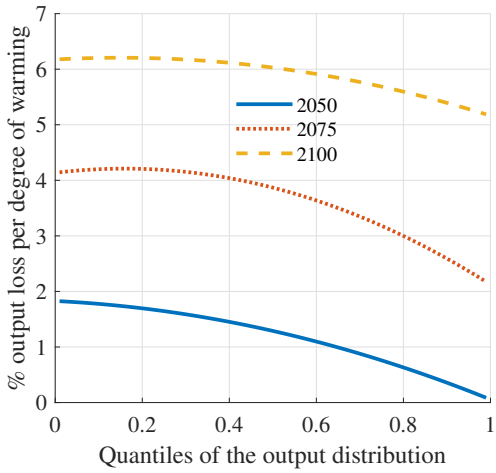

Notes. For each output quantile, output losses are percentage deviation from baseline, normalized by the corresponding temperature increase at each date.

time t are

$$l_q(t) = -\left(\frac{Y_q^{\text{bas}}(t)}{Y_q^{\text{alt}}(t)} - 1\right),$$

where $Y_q^{\text{bas}}(t)$ is the q-th quantile of output at time t in the baseline scenario, and $Y_q^{\text{alt}}(t)$ is its counterpart in the alternative scenario. To express output losses per degree Celsius, we use the linear link between atmospheric CO_2 and temperature from Matthews et al. (2009, 2012).[14] With this link, we compute

$$L_q(t) = 100 \times \frac{l_q(t)}{\Delta T(t)},$$

where $\Delta T(t)$ is the change in temperature between the initial year 2021 and year $t > 2021$.

Figure 5 reports reports output losses per degree of warming $L_q(t)$ for all output distribution quantiles $q \in [0.01, 0.99]$ and years $t = \{2050, 2075, 2100\}$. By 2100 the median country loses about 6 percent of output per additional degree Celsius, which is in the range of the empirical evidence presented in Section 2. Also in line with the data, poorer countries experience larger economic losses from climate change: at the end of the century, output losses at the 10th percentile are roughly one percentage point higher than at the 90th percentile.

In our model, this pattern arises as follows. Rising atmospheric CO_2 concentrations reduce the *common* growth rate of labor and labor-augmenting productivity. Countries respond

[14] More precisely, we compute the temperature increase caused by cumulative CO_2 emissions, $CE(t) = \epsilon \int_{t_0}^{t} A(u)N(u)\bar{x}(u)du$ using the linear relationship $\Delta T(t) = \chi CE(t)$. We set χ, the Carbon–Climate Response, to its standard value of 1.75°C per 1000 Gt of carbon (Matthews et al., 2009, 2012).

differently to this decline. High-income countries, with lower marginal utility of consumption, reduce current consumption to support capital accumulation. Lower-income countries, with higher marginal utility, are less willing to cut consumption, so capital accumulation suffers more. This generates a negative gradient in the economic costs of climate change across income levels.

Lastly, the costs of global warming rise over time, as higher atmospheric CO_2 reduces labor and productivity growth, producing cumulative effects.

Overall, the model is consistent with empirical regularities 1–6, with some caveats due to the assumed convergence to a unique steady state and the degenerate distribution of carbon intensity. These results give us confidence that the model provides a reliable quantitative laboratory for evaluating climate policy. Moreover, because the costs of global warming vary across countries and horizons, support for policy may also differ accordingly. We now turn to this question.

6. Global carbon tax

This section considers a global tax on fossil fuels, where domestic carbon tax revenues are redistributed lump sum to the representative household in each country. We address two questions. First, which countries would be willing to accept this scheme? Second, how does this willingness depend on the time horizon over which countries evaluate its effects?

6.1. **Impacts of the carbon tax.**

Suppose that countries purchasing fossil fuels from the extractor country face a proportional carbon tax, τ, which raises the effective price of fossil fuels to $(1+\tau)\,c_x$. In each country, the tax proceeds $m(t)$ are redistributed lump-sum to the representative household with $m(t) = \tau\, c_x\, x(t)$. As the elasticity of final output with respect to brown energy converges to zero when $t \to \infty$, both fossil fuel use and lump-sum transfers vanish asymptotically. As a result, the interior steady state of the MFG remains unchanged (see Appendix E.1 for details).

To calibrate the carbon tax rate τ, we follow Rennert et al. (2022), which reports a point estimate for the social cost of carbon of 157 (in 2010 USD per ton of CO_2), with a 95% confidence range between 37 and 351. According to the World Bank's Pink Sheet, in 2021, our initial year, the cost of a ton of CO_2 was 151 USD at constant 2010 prices.[15] Therefore,

[15]More precisely, according to the World Bank Pink Sheet, the 2021 price of Brent crude oil in 2010 USD was 64 dollars per barrel. Since a metric ton of oil corresponds to approximately 7.33 barrels, the price of one ton of oil was about 470 dollars. Crude oil consists primarily of hydrocarbons. When burned, the carbon in the fuel combines with oxygen to form CO_2. Because the molecular weight of CO_2 is higher than that

FIGURE 6. Output growth versus temperature rise across carbon tax scenarios

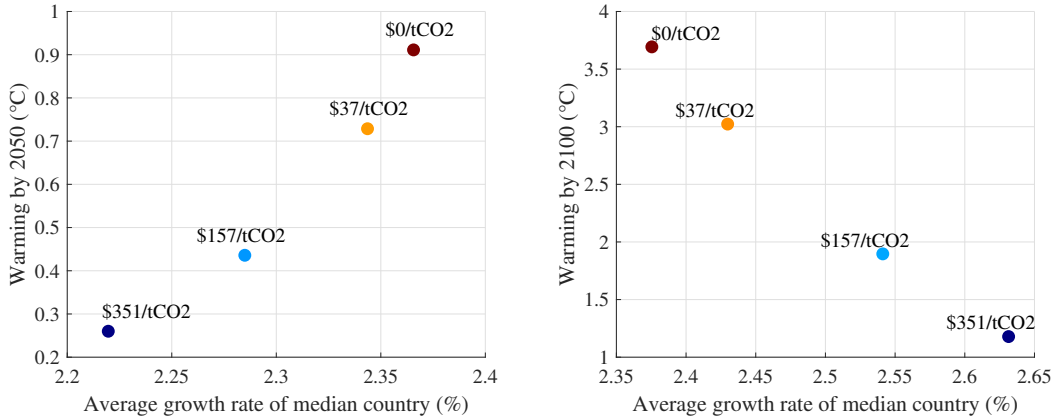

Notes. For the period between 2021 and 2050, the left panel plots the temperature increase against the compound average annual output growth in the median country, distinguishing four carbon tax levels taken from Rennert et al. (2022): 0, 37, 157 and 351 $/tCO$_2$ (constant 2010 prices). The right panel shows the corresponding relationship for the period between 2021 and 2100.

the calibrated tax rate is $\tau = \frac{157}{151} \approx 1.04$ with a 95% confidence range between 0.24 and 2.32.

The left panel of Figure 6 shows the relationship between the temperature increase from 2021 to 2050 and the compound average annual output growth in the median country over the same period.[16] It displays the baseline no-tax case and the three calibrated tax rates: 0.24 ($37/tCO$_2$), 1.04 ($157/tCO$_2$), and 2.32 ($351/tCO$_2$). The right panel considers a longer horizon, showing the corresponding relationship for the period 2021–2100. As expected, by raising the cost of fossil fuels, the global carbon tax reduces global CO_2 emissions, thereby limiting temperature increases over time. However, keeping temperature outcomes within acceptable bounds requires high tax levels; only the $351/tCO$_2$ carbon tax limits temperature increases to 0.25°C in 2050 and 1.2°C in 2100.

The impact of the carbon tax on growth is not monotonic over time. It dampens output growth in the first decades after implementation but enhances it over longer horizons. For example, setting the tax at $351/tCO$_2$ lowers the compound average annual output growth of the median country by about 15 basis points relative to the baseline between 2021 and 2050, but raises it by about 25 basis points over the horizon 2021–2100.

---

of elemental carbon, the combustion of one ton of oil generates about 3.1 tons of CO_2. Dividing 470 by 3.1 yields approximately 151 2010 USD per ton of CO_2.

[16] As before, we convert changes in atmospheric CO_2 into temperature increases using the linear mapping in Matthews et al. (2009, 2012), based on a Carbon-Climate Response parameter of 1.75°C per 1000 Gt of carbon.

Two opposing forces determine the net effect of the tax on growth, resulting in this non-monotonic pattern. On the one hand, the tax increases input costs, generating an effect comparable to a negative total factor productivity shock in the final goods sector: current output declines and capital accumulation slows, amplifying the initial impact.[17] On the other hand, by curbing global CO_2 emissions, the tax raises the global growth rate of labor and labor-augmenting productivity. At shorter horizons, the first effect dominates; at longer horizons, the second effect prevails.

6.2. **Willingness to pay.** The non-monotonic effects studied above suggest that a country's willingness to adopt the carbon tax depends on the time horizon over which it evaluates its effects. The outcome of this assessment will differ with the country's position in the income distribution too. To make this clearer, we compute a consumption-equivalent metric that measures the percentage change in baseline (no-tax) consumption that makes a country indifferent between the baseline and tax scenario. We allow this metric to vary with the time horizon over which countries assess the effects of the tax. Formally, at initial time t_0 and given capital level k, we consider the truncated value function at time horizon $T \geq 0$, defined as

$$v_T(t_0, k) = \int_{t_0}^{t_0+T} e^{-\rho(t-t_0)} \ln C(t) \, \mathrm{d}t \,,$$

with log utility as in our calibration (see Table 2) and where $C(t)$ denotes the optimal consumption path (non detrended), obtained by solving the HJB equation in Proposition 3. Appendix E.2 shows that the consumption-equivalent measure with a time horizon T is

$$\varphi_T(t_0, k) = \mathrm{e}^{\frac{\rho\left(v_T^{tax}(t_0,k) - v_T^{bas}(t_0,k)\right)}{1-\mathrm{e}^{-\rho T}}} - 1 \,,$$

where $v_T^{tax}(t_0, k)$ is the truncated value function under the carbon tax scenario, and $v_T^{bas}(t_0, k)$ is the truncated value function under the baseline scenario. The horizon $T \geq 0$ determines how far ahead each country evaluates the effects of the carbon tax.[18] When $T \to \infty$, the consumption-equivalent metric simplifies to

$$\varphi_\infty(t_0, k) = \mathrm{e}^{\rho\left(v_\infty^{tax}(t_0,k) - v_\infty^{bas}(t_0,k)\right)} - 1 \,.$$

[17] Formally, it is straightforward to show that a higher tax rate τ reduces the productivity parameter $\tilde{y}$ in equation (3).

[18] In other words, agents make decisions taking into account the entire discounted future, and our metric is computed ex post over different horizons T. An alternative approach would be to maintain an infinite horizon for the evaluation and instead vary the discount rate ρ. However, changing ρ would affect not only the steady state but also the transition dynamics. Matching the targeted moments would then require re-calibrating the full set of model parameters jointly with ρ.

FIGURE 7. Willingness to pay for a global carbon tax

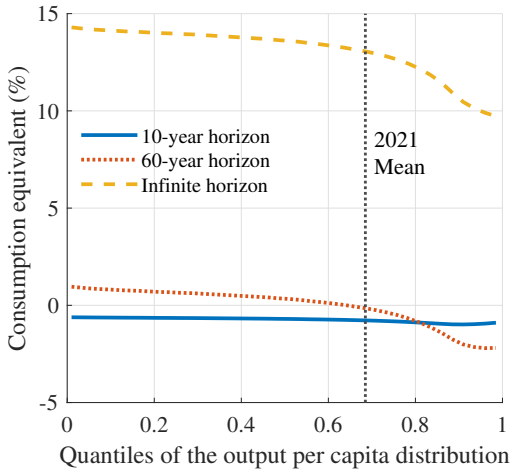

Notes. The consumption equivalent measures the percentage change in consumption in the baseline no-carbon-tax case that would make a country indifferent between the carbon-tax and the baseline. A positive value indicates a preference for the carbon-tax scenario. The three curves report welfare evaluated over a 10-year horizon, a 60-year horizon, and an infinite horizon. The carbon tax is set at \$351 per ton of CO_2 (constant 2010 prices).

Figure 7 plots the $t_0 = 1$ (corresponding to the year 2021) consumption-equivalent measure, $\varphi(t_0, k)$, for the tax scenario $\tau = 2.32$ (\$351/tCO_2) against countries' positions in the cross-sectional distribution of output per capita in 2021. We show three evaluation horizons: $T = 10$ years (solid blue line), $T = 60$ years (dotted red line), and $T \to \infty$ (dashed yellow line). Over a 10-year horizon, no country benefits from the global carbon tax. All countries experience a negative supply shock, while the positive effects of reduced warming have not yet materialized (see the left-hand side of Figure 6).

As the evaluation horizon lengthens, the willingness to pay for a global carbon tax rises. By lowering atmospheric CO_2, the carbon tax boosts growth in the long-run (see the right-hand side of Figure 6) and, in turn, countries' willingness to accept it. In the limit as $T \to \infty$, these gains are large: the median country would be willing to forgo 13% of its consumption at every instant to move from the baseline to the tax scenario.

Figure 7 also reveals an income gradient in the willingness to accept climate action, as in the data (see Figure 1). Over a 60-year horizon, corresponding to the remaining life expectancy of young adults, countries at the 5th percentile of the income distribution would be willing to forgo 0.9% of their consumption, whereas countries at the 95th percentile would require a 2.2% *increase* in consumption to accept the same policy. This gradient arises because poorer countries face larger economic damages from atmospheric CO_2, and therefore benefit more from climate mitigation. Figure 8 shows this pattern across all 134 countries in our sample

FIGURE 8. Willingness to pay for a global carbon tax over a 60-year horizon

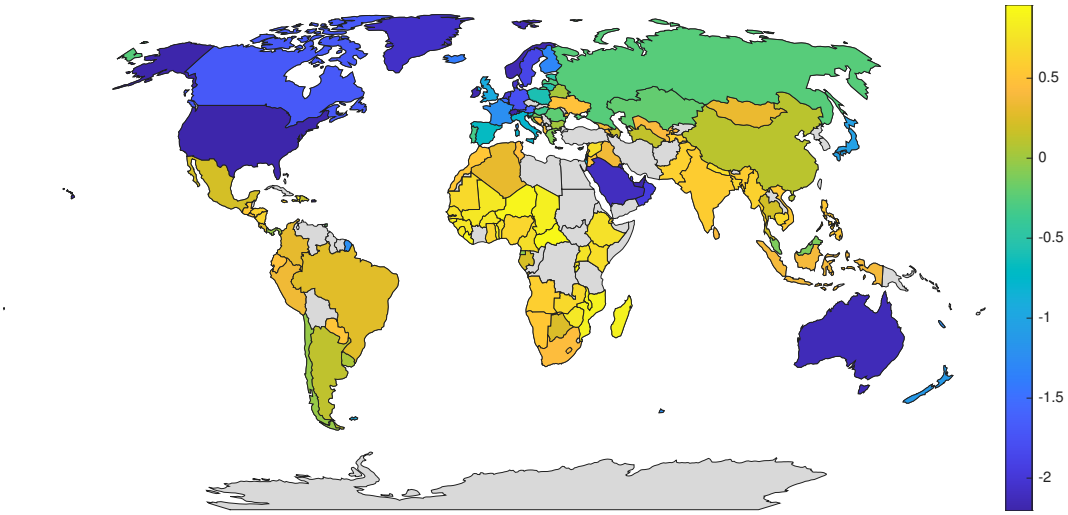

Notes. The consumption equivalent measures the percentage change in consumption in the baseline no-carbon-tax case that would make a country indifferent between the carbon-tax and the baseline. A positive value indicates a preference for the carbon-tax scenario. The map reports welfare evaluated over a 60-year horizon for a carbon tax at \$351 per ton of CO_2 (constant 2010 prices). Countries in gray are not included in our sample.

over the same 60-year horizon: poor countries (mainly in Central and South America, Africa, and parts of Asia) favor the carbon tax, China is neutral, and the richest countries in North America, Europe, the Arabian Peninsula, and parts of Oceania oppose it.

Our policy experiment casts doubt on a common explanation for the income gradient, namely that it reflects higher adaptation costs in richer countries because they emit more CO_2 (Andre et al., 2024). In our setup, richer countries do emit more CO_2, but emissions per unit of output are identical across countries, consistent with the almost flat relationship between carbon intensity and output in the data. A given carbon tax therefore entails the same output cost across countries. The income gradient in willingness to accept climate action thus need not stem from higher mitigation or adaptation costs in rich countries, but from greater climate damages in poorer ones.

Overall, Figures 7 and 8 stress the role of the income gradient in shaping (the lack of) international cooperation on climate policy. Even over a long 60-year horizon, when most countries would support a high carbon tax, the richest countries remain reluctant. For them, inaction is the rational response, which helps explain the practical difficulties of implementing global climate policies.

7. Discussion

Given high-income countries' reluctance toward the previous global carbon tax scheme, this section studies alternative mechanisms that could sustain their participation.

7.1. **International transfers.** We begin by redistributing global carbon tax revenues uniformly across countries instead of returning domestic revenues to domestic households. Because high-income countries emit more CO_2, this scheme generates lump-sum transfers from richer to poorer countries. Such transfers often feature in public debates, as low-income countries have contributed less to cumulative emissions yet face more severe climate damages.

Formally, let $g(t, x)$ denote the cross-sectional density of fossil fuel use x across countries at time t (Appendix C shows how to move from the cross-sectional density $u(t, k)$ for k to the density for any other variable). Total proceeds from the global carbon tax are

$$P(t) = \int_0^\infty \tau\, c_x\, x\, g(t, x)\, \mathrm{d}x = \tau\, c_x\, \mu_x(t)\,,$$

where $\mu_x(t)$ is the cross-sectional average of fossil fuel use at time t. These proceeds are redistributed uniformly across countries through lump-sum transfers, denoted by $m(t)$, assuming that the aggregate resource constraint

$$P(t) = \int_0^\infty m(t)\, u(t, k)\, \mathrm{d}k = m(t)$$

holds every period. As before, since the elasticity of final output with respect to brown energy converges to zero as $t \to \infty$, both fossil fuel use and lump-sum transfers vanish asymptotically (see Appendix E.3 for details). Figure 9a shows that, because high-income countries are net contributors while low-income countries are net recipients, cross-country redistribution steepens the negative income gradient. As a result, they weaken participation incentives for wealthy countries and hinder global cooperation.

This mechanism implies a counter-intuitive alternative: transfers from poorer to richer countries would flatten the income gradient and broaden support for the tax. Two objections arise. First, feasibility: low-income countries possess limited surplus resources, so any such transfers would be quantitatively small.[19] Second, equity: high-income countries account for the majority of cumulative emissions since the Industrial Revolution (for instance, the United States accounts for 24% of cumulative emissions, and the three largest European countries for 12%; see Appendix A.1). Requiring poorer countries to compensate richer ones

[19]For instance, our calculation suggests that over the 60-year horizon studied earlier, transferring resources from countries with a positive consumption-equivalent metric to bring their metric to zero would only make countries between the 65th and 80th percentiles willing to accept the global carbon tax scheme.

FIGURE 9. Willingness to pay for a global carbon tax

(A) Cross-country redistribution

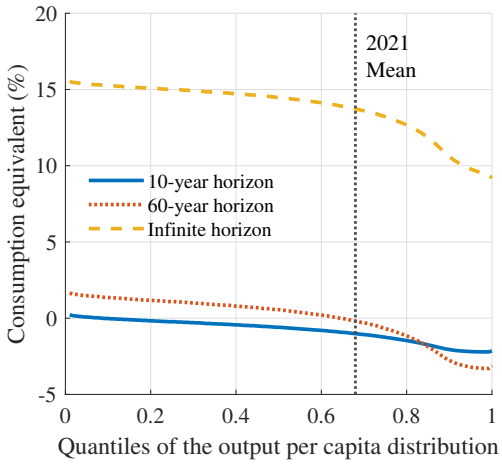

(B) Green capital subsidy

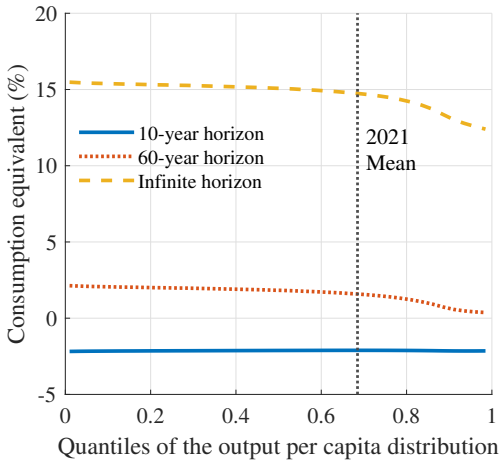

Notes. The consumption equivalent measures the percentage change in consumption in the baseline no-carbon-tax case that would make a country indifferent between the carbon-tax and the baseline. A positive value indicates a preference for the carbon-tax scenario. The three curves report welfare evaluated over a 10-year horizon, a 60-year horizon, and an infinite horizon. The carbon tax is set at \$351 per ton of CO_2 (constant 2010 prices).

would therefore conflict with widely endorsed principles of historical responsibility in climate policy.

7.2. **Subsidies to green capital.** In the short run, a carbon tax increases production costs, generating a negative supply shock. Would recycling tax revenues into subsidies for green capital investment offset this effect (see Ali et al., 2024, for related discussion)?

In our baseline model (see Section 3.1), the green energy sector incurs capital costs $r(t)k_g(t)$. Suppose these costs are subsidized, so that firms pay only $(1-\tilde{\tau}(t))\,r(t)k_g(t)$, where $\tilde{\tau}(t)$ denotes the subsidy rate. The subsidy is financed using domestic carbon tax revenues, implying a government budget constraint in each country

$$\tau c_x\, x(t) = \tilde{\tau}(t)\, r(t)k_g(t)\,.$$

The increase in production costs induced by the carbon tax is thus offset by the reduction in green capital costs generated by the subsidy. As before, as $x(t) \to 0$ asymptotically, the tax base shrinks and the subsidy rate $\tilde{\tau}(t)$ also converges to zero (see Appendix E.4 for details).

Figure 9b reports the resulting income gradient at different horizons. At a 60-year horizon, all countries support the carbon tax; at a 10-year horizon, no one does. In consumption-equivalent terms, the short-run loss for each country is about 2.5% with green finance, compared to 0.5% in the baseline scheme in Section 6. The difference arises because, in

the baseline, households receive tax revenues lump sum and can use them for current consumption, which mitigates welfare losses. With the green subsidy, households are induced to reallocate resources toward investment in clean technologies, reducing current consumption but increasing future productive capacity. Welfare is then lower in the short run but higher over longer horizons.

On the whole, neither international transfers nor alternative domestic recycling schemes ensure global support for carbon taxation in both the short and the long run. A stable agreement that remains acceptable over time likely requires more sophisticated international arrangements that support vulnerable countries while preserving participation incentives for major emitters (Bourles et al., 2025).

8. Robustness Checks

We now assess the robustness of our results to alternative calibration choices and model assumptions. In Sections 8.1 and 8.2, we examine how different calibrations of $\{\gamma, \kappa\}$ affect our findings. Section 8.3 relaxes the assumption of unit elasticity of substitution between brown and green energy by introducing a CES energy composite. Lastly, Section 8.4 considers an international capital market.

8.1. **Higher climate damages.** We face large uncertainty about the economic impact of global warming. Despite recent progress, evidence on the effects of higher average temperatures, rising sea levels, and more frequent and severe extreme weather events remains limited, both for economic outcomes and for societies more broadly (Pindyck, 2021). In light of this uncertainty, we revisit our global carbon tax scheme (without cross-country redistribution) by assuming larger climate damages. In particular, we double the damage parameter γ from 0.4 to 0.8. As a result, the median country loses about 12% of output per degree Celsius of warming by 2100.

As before, we study the consumption-equivalent measure $\varphi_T(t_0, k)$ at $t_0 = 1$ (year 2021) for the tax scenario $\tau = 2.32$ ($351/tCO$_2$), plotted against countries' positions in the cross-sectional distribution of output per capita in 2021. Figure 10 shows that the main qualitative insights remain unchanged. At the 10-year horizon, the consumption-equivalent profile is unchanged. All countries reject the carbon tax because at short horizons it acts as negative supply-shock. at longer horizons, the profile shifts upward relative to the baseline calibration, reflecting the larger benefits from curbing global CO_2 emissions.

8.2. **Faster energy transition.** Our model features green energy-biased technical progress, which raises the elasticity of final output with respect to green energy while reducing the elasticity with respect to brown energy (see Section 5.1). We capture the speed of this shift with the parameter κ, calibrated to match the twofold increase in the share of green energy

FIGURE 10. Willingness to pay a global carbon tax under higher climate damages

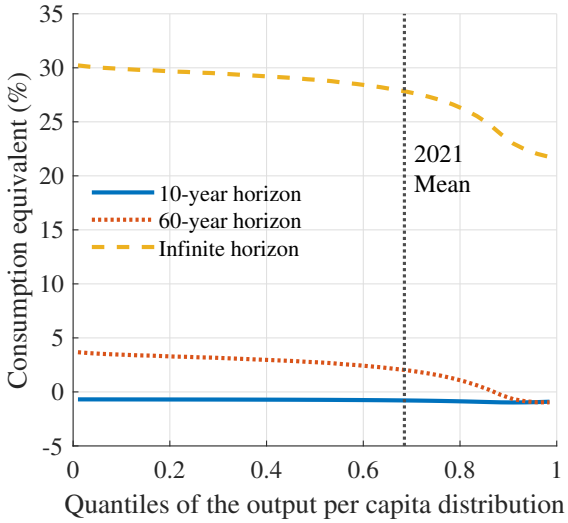

Notes. The consumption equivalent measures the percentage change in consumption in the baseline no-carbon-tax case that would make a country indifferent between the carbon-tax and the baseline. A positive value indicates a preference for the carbon-tax scenario. The three curves show welfare evaluated over a 10-year horizon, a 60-year horizon, and an infinite horizon. The carbon tax is set at \$351 per ton of CO_2 (constant 2010 prices).

in total energy use observed between 1990 and 2021. However, if we consider a larger value of κ, the decoupling of economic activity from fossil fuels accelerates, reducing the need for strict climate policy.

To illustrate, we double κ from 0.8 to 1.6. This lowers the elasticity of output with respect to brown energy in 2050 to about 1%, compared with 1.8% in the baseline. By 2075, the elasticity falls to 0.3%, versus 1.2% in the baseline, and it becomes virtually zero by the end of the century. In this scenario, our lowest carbon tax of \$37/tCO_2 delivers the same atmospheric CO_2 outcome, about 4,300 Gt, as our highest tax of \$351/tCO_2 in the baseline specification.

It seems unlikely that fossil fuels will become obsolete at the pace implied by $\kappa = 1.6$. Even if they did, the model suggests that a non-trivial carbon tax would still be required to keep temperature increases within acceptable bounds.

8.3. **Energy composite.** In the baseline model, the final goods sector uses a Cobb–Douglas production function. As a result, the elasticity of substitution between brown and green energy equals one, as in Acemoglu et al. (2012) and Rezai and van der Ploeg (2015). We now relax this assumption by introducing an energy composite $E(t)$ that aggregates brown

and green energy through a constant elasticity of substitution (CES) function.

$$E(t) = \left(\frac{\mu_f}{\mu_f + \nu_f} E_b(t)^r + \frac{\nu_f}{\mu_f + \nu_f} E_g(t)^r \right)^{\frac{1}{r}} ,$$

where $r \in (-\infty, 1]$ and the elasticity of substitution is $1/(1-r)$. When $r = 0$, the specification reduces to the Cobb–Douglas case (see Appendix F.1).

In this extended setup, the model can still be detrended and written as an MFG system (see Proposition 4 in Appendix F.1), though solving it is more challenging. In the baseline model with a Cobb-Douglas specification, all variables can be written as *explicit* functions of k. As a result, only k (the state variable) and c (the control variable) appear in the HJB equation in Proposition 3. Under a CES specification (with $r \neq 0$), variables can only be expressed as *implicit* functions of k. In other words, solving the HJB equation in Proposition 4 also requires the simultaneous solution of a system of non-linear equations for each given pair (t, k).

Finally, as discussed in Section 5.2, a Cobb-Douglas specification (that is, a CES with $r = 0$, or equivalently a unit elasticity of substitution between brown and green energy) implies that carbon intensity is constant across the distribution of countries (see the solid blue line in Figure 11). When the elasticity of substitution differs from one, carbon intensity is no longer constant across countries. More precisely, when the elasticity is below one (dotted red line), carbon intensity increases with output, whereas the opposite pattern emerges when the elasticity exceeds one (dashed yellow line). Quantitatively, however, these effects are weak.[20]

8.4. **International capital market.** Following the seminal Nordhaus multi-region integrated assessment model RICE, Hassler and Krusell (2012) and many others, our baseline model includes international trade in fossil fuels but abstracts from trade in other commodities. As a result, household assets within each country equal firm capital, which simplifies the solution of the model. In this subsection, we introduce an international capital market. A given country's assets, $a(t)$, may then differ from its capital input, $k(t)$. This implies a world interest rate, $r(t)$, which adjusts to satisfy the market-clearing condition

$$\int_0^\infty a\, u(t,a)\, \mathrm{d}a = \int_0^\infty k\, u_k(t,k)\, \mathrm{d}k\,.$$

Here $u(t,a)$ and $u_k(t,k)$ denote the cross-country distributions of assets and capital. We assume that assets and capital are positive. Without an additional mechanism, all countries would choose the same level of capital input and thus the same output. To prevent this, we follow Schmitt-Grohe and Uribe (2003) and introduce a debt-elastic interest rate premium.

[20]Note that the average level of carbon intensity also varies with the elasticity of substitution. We could hold it constant by recalibrating μ_b (see Table 2).

FIGURE 11. Carbon intensity across output per capita in 1990

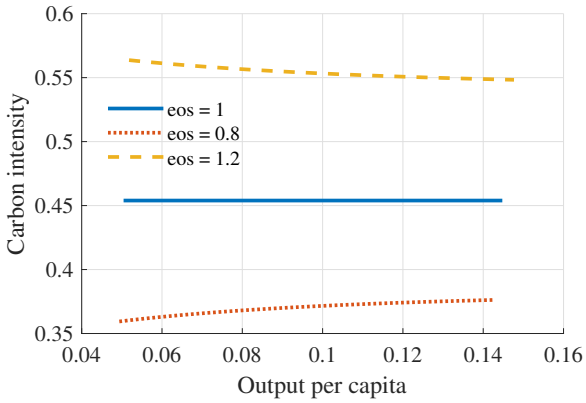

Notes. The figure shows carbon intensity as a function of output per capita for different levels of the elasticity of subsitution (eos) between brown and green energy. The solid blue line eos=1 corresponds to the Cobb-Douglas specification in our baseline model.

FIGURE 12. Assets and capital, 1990

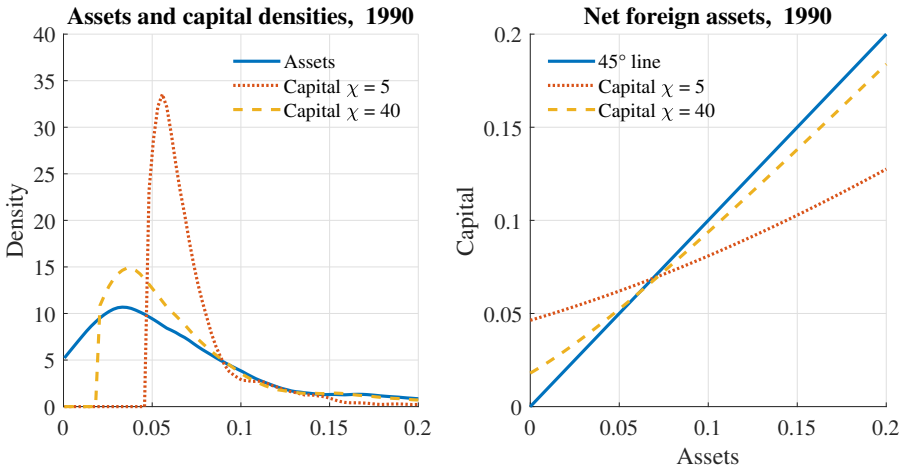

Notes. The left-hand side figure compares the cross-sectional densities of per capita assets and capital in 1990. The density of assets is imposed as an initial condition, and the density of capital is obtained from the model for $\chi = 5$ and $\chi = 40$, where parameter χ governs the elasticity of the interest rate with respect to the net foreign asset position. The right-hand side figure plots capital as a function of assets. When the capital line is below the 45° line, net foreign assets are positive.

That is, a country's interest rate, $\tilde{r}(t)$, depends on the world interest rate, $r(t)$, and on its net foreign asset position, $nfa(t) = a(t) - k(t)$,

$$\tilde{r}(t) = r(t)\, \mathrm{e}^{-\chi\, nfa(t)}\,,$$

where $\chi \geq 0$. Firms in countries with negative net foreign assets then face a higher borrowing rate than firms in countries with positive net assets.

The asymptotic properties of the model remain unchanged: a unique and stable steady state exists. Furthermore, the model can still be written as a MFG system, as shown in Proposition 5 in Appendix F.2. As a matter of fact, when $\chi \to \infty$, $k(t) = a(t)$ and the model reduces to our baseline specification. In contrast, when $\chi \to 0$, $\tilde{r}(t) = r(t)$. Firms in all countries then face the same borrowing rate and choose the same level of capital and output.[21]

Solving the model with international trade in capital poses a new challenge: at each instant t, we must find the world interest rate $r(t)$ that clears the capital market. For numerical tractability, we remove the aggregate-demand externality, so that productivity in the final good sector is constant and common to all countries. This ensures a one-to-one link between a country's assets and its capital input. To illustrate the numerical properties of the extended model, we consider two values for the interest rate premium parameter, $\chi = 5$ and $\chi = 40$. Though arbitrary, $\chi = 5$ implies that a country with net foreign assets equal to 50% of GDP receives an interest rate discount of 0.25% relative to a country with zero net assets. For $\chi = 40$, the discount is 2%.

The left panel of Figure 12 compares the initial distribution of capital inputs for these two values of χ. As χ rises, the extended model converges to the baseline specification, with the capital distribution moving closer to the asset distribution. As χ falls, borrowing rates become more similar across countries, and the latter choose the same capital input. The right panel of Figure 12 shows that countries with low initial asset holdings start with negative net foreign asset positions. Since net foreign assets equal zero in the steady state, these countries must run trade surpluses over time. The opposite holds for countries with high initial asset holdings. Lastly, allowing for international trade in capital has only minor effects on aggregate variables. Between 1990 and 2021, atmospheric CO_2 increases by 26% if $\chi = 5$, 25% if $\chi = 40$, and 23% in our baseline model ($\chi \to \infty$). All previous insights on climate policy carry over to the extension with international trade in capital.

9. Concluding Remarks

We study a heterogeneous-country integrated assessment model in continuous time with a continuum of countries. The model combines neoclassical growth with climate damages that reduce productivity growth and captures cross-country differences in capital, output,

[21]For the model with international trade in capital to be well-defined, the function $F(\cdot)$ linking assets and capital, $a(t) = F(k(t))$, must be bijective. With the aggregate-demand externality, where total factor productivity depends on capital, this property might have to be verified numerically. See Appendix F.2 for details.

and energy use. Our setup aligns with a wide range of empirical regularities, including the negative correlation between national income and the economic costs of climate change.

Using this framework as a quantitative laboratory, we evaluate a global carbon tax and its distributional implications. Our results reveal a clear income gradient in the willingness to accept climate action: poorer countries benefit more from mitigating climate damages and are more willing to adopt the tax, while rich countries are more reluctant. Cross-country redistribution of carbon-tax revenues, intended to compensate low-income countries, steepens this gradient, highlighting the challenges of designing effective international climate agreements.

Several extensions could broaden the framework. A key challenge is generating persistent cross-country heterogeneity. In the baseline, we capture this through an aggregate-demand externality; an alternative is to introduce stochastic productivity shocks, which would produce a stationary distribution in the long run and convert the first-order partial differential equations in the MFG into second-order equations. Richer structures, such as non-unitary elasticities of substitution between brown and green capital or international capital trade, could also be incorporated, though solving the resulting equilibrium would be more demanding. Full quantitative analysis of these extensions is left for future work.

References

Acemoglu, D. (2009). *Introduction to modern economic growth*. Princeton Univ. Press, Princeton, NJ.

Acemoglu, D., Aghion, P., Bursztyn, L., and Hemous, D. (2012). The Environment and Directed Technical Change. *American Economic Review*, 102(1):131–166.

Acemoglu, D., Akcigit, U., Hanley, D., and Kerr, W. (2016). Transition to Clean Technology. *Journal of Political Economy*, 124(1):52–104.

Achdou, Y., Han, J., Lasry, J.-M., Lions, P.-L., and Moll, B. (2022). Income and wealth distribution in macroeconomics: A continuous-time approach. *The Review of Economic Studies*, 89(1):45–86.

Aid, R., Federico, S., Ferrari, G., and Rodosthenous, N. (2025). Regulation in a mean-field investment game with climate damage. *Center for Mathematical Economics Working Papers, No. 705, Bielefeld University, Center for Mathematical Economics (IMW), Bielefeld*.

Ali, M., Seraj, M., Turuc, F., Tursoy, T., and Uktamov, K. F. (2024). Green finance investment and climate change mitigation in OECD-15 European countries: RALS and QARDL evidence. *Environment, Development and Sustainability: A Multidisciplinary Approach to the Theory and Practice of Sustainable Development*, 26(11):27409–27429.

Andre, P., Boneva, T., Chopra, F., and Falk, A. (2024). Globally representative evidence on the actual and perceived support for climate action. *Nature Climate Change*, 14(3):253–259.

Archer, D. (2005). Fate of fossil fuel CO2 in geologic time. *Journal of Geophysical Research: Oceans*, 110(C9).

Bai, Y., Ríos-Rull, J.-V., and Storesletten, K. (2025). Demand shocks as technology shocks. *The Review of Economic Studies*, page rdaf045.

Bilal, A. and Kanzig, D. R. (2024). The macroeconomic impact of climate change: Global vs. local temperature. NBER Working Papers 32450, National Bureau of Economic Research, Inc.

Bodson, M. (2020). Explaining the Routh–Hurwitz Criterion: A Tutorial Presentation [Focus on Education]. *IEEE Control Systems Magazine*, 40(1):45–51.

Bourles, R., Laurent-Lucchetti, J., and Rochet, J. (2025). Dp20863 should we stop the cops? Discussion Paper 20863, CEPR, Paris & London.

Burke, M., Hsiang, S. M., and Miguel, E. (2015). Global non-linear effect of temperature on economic production. *Nature*, 527(7577):235–239.

Chang, J.-J., Mi, Z., and Wei, Y.-M. (2023). Temperature and GDP: A review of climate econometrics analysis. *Structural Change and Economic Dynamics*, 66:383–392.

De Nardi, M., Pashchenko, S., and Porapakkarm, P. (2024). The lifetime costs of bad health. *The Review of Economic Studies*.

Dell, M., Jones, B. F., and Olken, B. A. (2012). Temperature shocks and economic growth: Evidence from the last half century. *American Economic Journal: Macroeconomics*, 4(3):66–95.

Den Haan, W. J. (1997). Solving dynamic models with aggregate shocks and heterogeneous agents. *Macroeconomic Dynamics*, 1(2):355–386.

Deschênes, O. and Greenstone, M. (2011). Climate Change, Mortality, and Adaptation: Evidence from Annual Fluctuations in Weather in the US. *American Economic Journal: Applied Economics*, 3(4):152–85.

Feenstra, R. C., Inklaar, R., and Timmer, M. P. (2015). The Next Generation of the Penn World Table. *American Economic Review*, 105(10):3150–3182.

Fernandez-Villaverde, J., Rubio-Ramirez, J., and Schorfheide, F. (2016). Solution and Estimation Methods for DSGE Models. In Taylor, J. B. and Uhlig, H., editors, *Handbook of Macroeconomics*, volume 2, pages 527–724. Elsevier.

Garcia, P., Jacquinot, P., Lenarcic, C., Mavromatis, K., Papadopoulou, N., and Silgado-Gomez, E. (2026). Green transition in the euro area: Domestic and global factors. *European Economic Review*, 182:105206.

Garcia, P. and Pierrard, O. (2025). Modeling the Evolution of Carbon Intensity: Linking the Solow Model to the Transport Equation. *Forthcoming in Environmental and Resource Economics*.

Geruso, M. and Spears, D. (2018). Heat, Humidity, and Infant Mortality in the Developing World. NBER Working Papers 24870, National Bureau of Economic Research, Inc.

Golosov, M., Hassler, J., Krusell, P., and Tsyvinski, A. (2014). Optimal Taxes on Fossil Fuel in General Equilibrium. *Econometrica*, 82(1):41–88.

Graff Zivin, J. and Neidell, M. (2012). The Impact of Pollution on Worker Productivity. *American Economic Review*, 102(7):3652–73.

Hassler, J. and Krusell, P. (2012). Economics and climate change: Integrated assessment in a multi-region world. *Journal of the European Economic Association*, 10(5):974–1000.

Hassler, J., Krusell, P., and Olovsson, C. (2025). Climate policy in the wide world. *Econometrica*. Conditional accept.

Hassler, J., Krusell, P., and Smith, A. (2016). Environmental Macroeconomics. In Taylor, J. B. and Uhlig, H., editors, *Handbook of Macroeconomics*, volume 2, pages 1893–2008. Elsevier.

Heer, B. and Maußner, A. (2024). *Dynamic General Equilibrium Modeling*. Springer Texts in Business and Economics. Springer Cham, 3rd edition.

Hillebrand, E. and Hillebrand, M. (2019). Optimal climate policies in a dynamic multi-country equilibrium model. *Journal of Economic Theory*, 179:200–239.

Hillebrand, E. and Hillebrand, M. (2023). Who pays the bill? Climate change, taxes, and transfers in a multi-region growth model. *Journal of Economic Dynamics and Control*,

153(C).

Kaplan, G. and Menzio, G. (2016). Shopping externalities and self-fulfilling unemployment fluctuations. *Journal of Political Economy*, 124(3):771–825.

Kotlikoff, L., Kubler, F., Polbin, A., and Scheidegger, S. (2024). Can today and tomorrow world uniformly gain from carbon taxation? *European Economic Review*, 168(C):None.

Krueger, D., Mitman, K., and Perri, F. (2016). Macroeconomics and Household Heterogeneity. In Taylor, J. B. and Uhlig, H., editors, *Handbook of Macroeconomics*, volume 2, pages 843–921. Elsevier.

Krusell, P. and Smith, A. A. (1998). Income and Wealth Heterogeneity in the Macroeconomy. *Journal of Political Economy*, 106(5):867–896.

Mankiw, N. G., Romer, D., and Weil, D. N. (1992). A Contribution to the Empirics of Economic Growth. *The Quarterly Journal of Economics*, 107(2):407–437.

Matthews, H. D., Gillett, N. P., Stott, P. A., and Zickfeld, K. (2009). The proportionality of global warming to cumulative carbon emissions. *Nature*, 459(7248):829–832.

Matthews, H. D., Solomon, S., and Pierrehumbert, R. (2012). Cumulative carbon as a policy framework for achieving climate stabilization. *Philosophical Transactions of the Royal Society A: Mathematical, Physical and Engineering Sciences*, 370(1974):4365–4379.

Nath, I. B., Ramey, V. A., and Klenow, P. J. (2024). How much will global warming cool global growth? NBER Working Papers 32761, National Bureau of Economic Research, Inc.

Newell, R. G., Prest, B. C., and Sexton, S. E. (2021). The GDP-Temperature relationship: Implications for climate change damages. *Journal of Environmental Economics and Management*, 108:102445.

OECD (2016). *The Economic Consequences of Outdoor Air Pollution*. OECD Publishing, Paris.

Olver, P. J. (2014). *Introduction to Partial Differential Equations*. Springer International Publishing, 2014 edition.

Pindyck, R. S. (2021). What We Know and Don't Know about Climate Change, and Implications for Policy. *Environmental and Energy Policy and the Economy*, 2(1):4–43.

Rennert, K., Errickson, F., Prest, B. C., et al. (2022). Comprehensive evidence implies a higher social cost of CO2. *Nature*, 610:687–692.

Rezai, A. and van der Ploeg, F. (2015). Robustness of a simple rule for the social cost of carbon. *Economics Letters*, 132:48–55.

Romer, P. (1989). Capital accumulation in the theory of long run growth. In Barro, R. J., editor, *Modern Business Cycle Theory*, pages 51–127. Harvard University Press, Cambridge, MA.

Schmitt-Grohe, S. and Uribe, M. (2003). Closing small open economy models. *Journal of International Economics*, 61(1):163–185.

Shampine, L. F., Gladwell, I., and Thompson, S. (2003). *Solving ODEs with MATLAB*. Cambridge University Press.

van den Bremer, T. S. and van der Ploeg, F. (2021). The risk-adjusted carbon price. *American Economic Review*, 111(9):2782–2810.

Zhao, X., Hu, L., Chen, X., and Ling, L. (2026). Energy-biased technological progress and green innovation: Evidence from Chinese cities. *Renewable Energy*, 256:124079.

TABLE 4. Data sources

Series	Source	Coverage
WTC 1% of income	Global Climate Change Survey	Country-level
CO_2 emissions	Emissions Database for Global Atmospheric Research	Country-level
Population	Maddison Project Database 2023	Country-level
Real GDP per capita	Maddison Project Database 2023	Country-level
CO_2 in Earth's atmosphere	National Oceanic and Atmospheric Administration	Global
Real capital stock	Penn World Table 10.01	Country-level
Share of labour compensation in GDP	Penn World Table 10.01	Country-level
Crude oil, Brent	World Bank Commodity Price Data (The Pink Sheet)	Global
Oil, coal and gas consumption	Energy Institute Statistical Review of World Energy 2025	Global
Alternative and nuclear energy	International Energy Agency	Country-level
Energy use	International Energy Agency	Country-level
Income classification	World Bank	Country-level
Levelised cost of green energy	International Renewable Energy Agency	Global
Employment in mining and utilities	International Labour Organization	19 high-income econ.
Cumulative CO_2 emissions since 1750	Global Carbon Budget (2024)	Country-level

Notes. The Global Climate Change Survey is presented in Andre et al. (2024). Data on levelised cost of green energy and oil, coal and gas consumption processed by `ourworldindata.org`. Data on energy use from the World Bank DataBank. Mining and utilities covers employment in mining, quarrying, electricity, gas, and water supply. Data on cumulative CO_2 emissions processed by `https://ourworldindata.org/data-insights/which-countries-have-contributed-the-most-to-historical-co-emissions`.

APPENDIX A. DATA AND CALIBRATION

A.1. **Data.** Table 4 lists the series used in this paper. For all cross-country variables, we work with a sample of 134 countries spanning the period 1990-2021, except for the real capital stock variable, which is available until 2019. We do not have sufficient data for the other countries but they only represent a few percent of the world GDP (see Figure 8 for an overview of missing countries). Of our 134 countries, 50 are classified as high-income economies, which we use to compute certain medians in the calibration process. All data sources are publicly available.

A.2. **Calibration.**

A.2.1. *Units.* we use the following abbreviations: \$ for US dollar (constant 2011 prices), t for ton, g for gram, Wh for watt-hour, k for kilo (10^3), G for giga (10^9), T for tera (10^{12}), and n is a normalization constant.

Several parameters are unit free: the functional parameters $\{\sigma, \kappa, \beta_f, \beta_g\}$, the elasticities $\{\mu_{f0}, \nu_{f0}, \alpha_f, \mu_b, \alpha_g, \alpha_b\}$, initial levels $\{A(0), N(0)\}$, the initial density $u_0(k)$ and the share λ. All rate parameters $\{\rho, \delta, p_0, \psi\}$ are expressed in $1/\Delta t$ unit. To fix the units of the parameters $\{s_0, \epsilon, c_x, \gamma\}$, we make three assumption: (1) the variable $S(t)$ is expressed in nGt of CO_2, (2) the variable $X(t)$ is expressed in Tt of fossil fuel/Δt, and (3) the carbon intensity is expressed in kg of CO_2/\$. Therefore s_0 is in nGt of CO_2. Using equation $\dot{S}(t) = \epsilon \bar{X}(t) - \psi S(t)$ from

Appendix B.4, we obtain that ϵ is in nt of CO_2/kt of fossil fuel. Carbon intensity is defined as $\epsilon X(t)/Y(t)$. From Appendix B.4, we also have $X(t)/Y(t) = \mu_f(t)\mu_b/c_x$. Then c_x is in $n\$/\text{t}$ of fossil fuel. Finally, we obtain that γ is in $1/\Delta t$ from the last equation in Appendix B.4.

Determining the units of the TFP parameters $\{\theta_g, \theta_b, \theta_{f0}\}$ is more complex. To do so, we first assume that energy $E_g(t)$ and $E_b(t)$ are in $\text{TWh}/\Delta t$. We then observe that $\mu_f(t)\mu_b Y(t) = c_x X(t)$, meaning that $Y(t)$ is in $n\text{T}\$/\Delta t$ and all $K(t)'s$ are in $n\text{T}\$$. Finally, h denotes one unit of non-detrended hours. Using the production functions (see Appendix B.1), we obtain

$$\begin{aligned}
\theta_g \;&\text{ in }\; \frac{\text{TWh}}{\Delta t}\left(\frac{1}{n\text{T}\$}\right)^{\alpha_g}\left(\frac{1}{\text{h}}\right)^{1-\alpha_g}, \\
\theta_b \;&\text{ in }\; \frac{\text{TWh}}{(\Delta t)^{1-\mu_b}}\left(\frac{1}{n\text{T}\$}\right)^{\alpha_b}\left(\frac{1}{\text{Tt fossil fuel}}\right)^{\mu_b}\left(\frac{1}{\text{h}}\right)^{1-\alpha_b-\mu_b}, \\
\theta_{f0} \;&\text{ in }\; \frac{(n\text{T}\$)^{1-\alpha_f}}{(\Delta t)^{1-\mu_{f0}-\nu_{f0}}}\left(\frac{1}{\text{TWh}}\right)^{\mu_{f0}+\nu_{f0}}\left(\frac{1}{\text{h}}\right)^{1-\alpha_f-\mu_{f0}-\nu_{f0}}.
\end{aligned}$$

From this, we can easily recover the units of aggregate parameters in Definition 1. In particular, $\{\mu, \alpha\}$ are unit free, ϕ is in kg of $CO_2/\$$, and

$$\tilde{y} \;\text{ in }\; \frac{\left(\frac{n\text{T}\$}{\text{h}}\right)^{\frac{\mu-\alpha}{\mu}}}{\Delta t}.$$

A.2.2. *Representative household.* We normalize one time unit to 32 years ($\Delta t = 32$). Assuming an annual real interest rate of 1% (or equivalently, a discount factor of 0.99, see for instance Golosov et al., 2014; Hillebrand and Hillebrand, 2019) yields a discount rate parameter ρ determined as

$$\text{e}^{-\rho} = 0.99^{\Delta t}.$$

We set the inverse IES to $\sigma = 1$, a standard value in macroeconomics (Golosov et al., 2014; Hillebrand and Hillebrand, 2019). Additionally, we take an annual capital depreciation rate of 6% (see e.g., Romer, 1989; Mankiw et al., 1992), and we obtain δ as

$$\text{e}^{-\delta} = (1 - 0.06)^{\Delta t}.$$

Finally, we assume that total growth is split according to $n(t) = \lambda p(t)$, with $\lambda = 0.5$.

A.2.3. *Initial conditions.*

Atmospheric CO_2. In January 1990, atmospheric CO_2 at the Mauna Loa Observatory was 356 parts per million (National Oceanic and Atmospheric Administration), equivalent to 2,760 gigatons (Gt) of CO_2. We normalize this initial concentration to one, $s_0 = 1$, which implies a normalization constant of $n = 2,760$.

Growth rate. We impose that, in the absence of climate damages (as we assume to be the case in 1990), the combined growth rate of labor and labor-augmenting technological progress is 4% (see Garcia and Pierrard, 2025, for empirical justifications), and we obtain p_0 as

$$\mathrm{e}^{p_0} = (1 + 0.04)^{\Delta t}.$$

In addition, we normalize the initial labor force and labor-augmenting technological progress to 1: $A(0) = N(0) = 1$ (see Proposition 1).

Capital probability density function. Assumption 1 imposes that countries differ in their initial capital stocks k_0, with $u(0, k) = u_0(k)$ the initial probability density function. We construct the empirical counterpart of $u_0(k)$ as follows. First, using the Penn World Table (Feenstra et al., 2015), we compute the ratio z_0 of physical capital to GDP in 1990 for a sample of 134 countries. In the model, this ratio has units $1/\Delta t$, so we convert the empirical values by multiplying each observation by 1/32. Second, in the model, the following identity holds (see Appendix B.3)

$$\frac{y(t)}{k(t)} = \tilde{y} k(t)^{\frac{\alpha-\mu}{\mu}}.$$

Therefore

$$z_0 \coloneqq \frac{k(0)}{y(0)} = \frac{k_0^{\frac{\mu-\alpha}{\mu}}}{\tilde{y}}, \quad \text{so that} \quad k_0 = (\tilde{y} z_0)^{\frac{\mu}{\mu-\alpha}},$$

where $\{\alpha, \mu, \tilde{y}\}$ are as in Definition 1. This gives, for each country, k_0 as a function of z_0, conditionally to the value of parameters $\{\alpha, \mu, \tilde{y}\}$, which are derived below. Third, we approximate the resulting distribution $u_0(k)$ of k_0 by a kernel distribution with an Epanechnikov kernel $\mathcal{K}(\cdot)$. Note that, for later use, the mean of this initial distribution is $k_{0,\mu} = 0.07$.

A.2.4. *Climate determinants.*

Fossil fuel extraction. Throughout the calibration, fossil fuel prices are proxied by the price of Brent crude oil, as reported by the World Bank Commodity Price Data (The Pink Sheet). This is a reasonable choice: in constructing its energy price index, the World Bank assigns an 85% weight to oil, 10% to natural gas, and 5% to coal. In 1990, the price of a barrel of Brent crude oil was 28 U.S. dollars in 2011 constant prices, equivalent to 205 dollars per ton of oil. For consistency with the climate block parameters, c_x must be expressed in units of $\frac{n\,\$}{\text{t oil}}$, where n is the normalization constant introduced above. We thus have $c_x = 205/n \approx 0.07$.

Emission factor. The emission factor ϵ converts fossil fuel use into CO_2 emissions. We source global fossil fuel consumption by type (oil, coal, gas) from 1990 to 2021 in the Energy Institute - 2025 Statistical Review of World Energy. Original data in terawatt-hour (TWh) are converted to gigajoules (GJ) via 1 TWh $= 3.6 \times 10^3$ GJ. Then using the energy content per ton of coal, gas, and oil (approx. 29.5, 53.6, 41.9 GJ), we compute total consumption in Gt. Figure 13 shows the results.

FIGURE 13. Global fossil fuel consumption

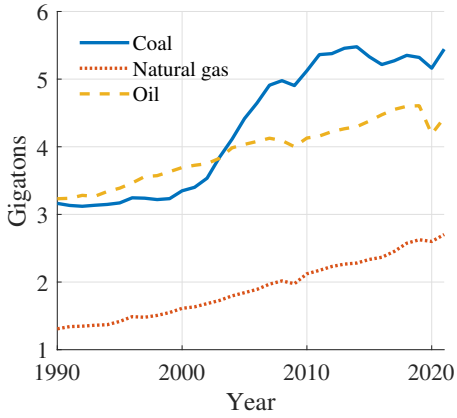

Notes. Global fossil fuel consumption by type (oil, coal, gas) from the Energy Institute - 2025 Statistical Review of World Energy, 1990-2021.

Next, we compute the carbon emitted by burning each fossil fuel, using standard carbon content figures: burning one ton of coal, gas, and oil emits roughly 2.9, 3, and 3.1 tons of CO_2.[22] Considering that the shares of coal, gas and oil in total fossil fuels are stable across time and represents 40%, 40% and 20% (see Figure 13), we obtain that 1 ton of 'aggregate' fossil fuel emits 3 tons of CO_2. We finally express this emission factor in model units ($\frac{n \text{ t CO2}}{\text{kt fossil fuel}}$), which gives $\epsilon = 3 \times 1000/n \approx 1.08$.

Decay rate ψ of atmospheric CO_2. Archer (2005) reports that approximately 80% of an excess atmospheric carbon concentration is removed after 300 years, while Golosov et al. (2014) calibrate their model so that 75% of an emitted unit of carbon is gone after 356 years. We follow Archer (2005) and, in our model notation, it means $e^{-\psi \times 300/\Delta t} = 20\%$, which implies $\psi \approx 0.17$.

Damage parameter. Calibrating the economic damages of climate change is challenging and uncertain (Newell et al., 2021). Uncertainty is compounded by the fact that rich and poor countries may face different consequences of global warming. For instance, Dell et al. (2012), find that GDP growth in rich countries is mostly unaffected by temperature, while poor countries experience adverse effects from positive temperature shocks. Specifically, they estimate that each additional 1°C of warming reduces annual GDP growth in poor economies by 1.4 percentage points. In contrast, Burke et al. (2015) argue that global warming hampers

[22]Burning one ton of fossil fuel produces more than one ton of carbon dioxide because each carbon atom combines with two oxygen atoms from the air.

economic growth in both rich and poor countries. They project that unmitigated warming could lower average global incomes by about 23% by 2100.

Because of uncertainty, we must make a somewhat arbitrary choice. We assume that all countries suffer from damage and that the combined annual growth of labor and labor-augmenting productivity falls by 0.5 percentage points per 1°C increase in temperature. This number is below Dell et al. (2012), but they only consider an effect on poor economies; and implies that a 1°C increase lowers output by 22% after 50 years, in the range of Burke et al. (2015).

With this target in hand, we proceed in three steps. First, we use the linear relationship between cumulative CO_2 emissions and global temperature from Matthews et al. (2009, 2012) to estimate the emissions required to raise the temperature by 1°C. This implies that cumulative CO_2 emissions must increase by 2,100 Gt. Assuming an airborne fraction of 50%, the corresponding rise in atmospheric CO_2 is 1,050 Gt. Taking 1990 as the initial year, this represents a relative increase of $\Delta S(t)/S(t) = 1050/2760 \approx 38\%$ to produce a 1°C temperature increase. Second, a reduction in annual growth of 0.5 percentage points implies, in our model's unit, that

$$\mathrm{e}^{\Delta p(t)} = (1 - 0.005)^{\Delta t}\,,$$

which yields $\Delta p(t) = -0.6$. Third, we combine these 2 numbers in a discretized version of equation (2)

$$\Delta p(t) = -\gamma \frac{\Delta S(t)}{S(t)}\,,$$

to get $\gamma = 0.42$. Given the uncertainty around this number, we conduct extensive robustness later.

A.2.5. *Production sectors.*

Elasticities of final output with respect to energy. Between 1990 and 2021, the median share of alternative and nuclear energy in total energy use increased by a factor of 2.6 across 134 countries and by a factor of 1.9 across a sub-sample of 50 high-income countries, as classified by the World Bank.[23] To capture this trend, we assume the following logistic functions (see Section 5.1 for references and properties)

$$\mu_f(t) = \frac{\mu_{f0} + \nu_{f0}}{1 + \frac{\nu_{f0}}{\mu_{f0}}\,\mathrm{e}^{\kappa t}}\,, \qquad \nu_f(t) = \frac{\mu_{f0} + \nu_{f0}}{1 + \frac{\mu_{f0}}{\nu_{f0}}\,\mathrm{e}^{-\kappa t}}\,.$$

To calibrate $\{\mu_{f0}, \nu_{f0}\}$, we observe that, given the Cobb–Douglas production structure, they determine the shares of brown and green energy expenditures in output at $t = 0$. To compute their empirical counterparts, we focus on high-income countries, since data coverage is more complete for this subgroup. Using fragmented data for the world as a whole, however, yields

[23] Source: World Bank DataBank, Alternative and nuclear energy (% of total energy use), EG.USE.COMM.CL.ZS.

FIGURE 14. Energy prices and use across high income economies

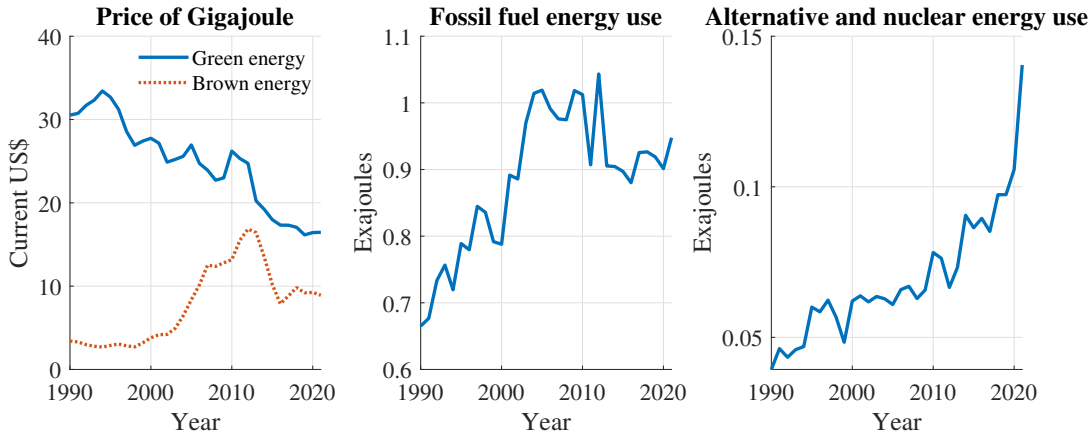

Notes. In the left panel, brown energy prices are proxied by the Brent crude oil price (World Bank Commodity Price Data, The Pink Sheet). Green energy prices are proxied by the median of the levelized cost of bio-energy, geothermal, offshore wind, solar photovoltaic, concentrated solar power, hydro-power, and onshore wind (International Renewable Energy Agency). The center and right panels show median fossil fuel and alternative/nuclear energy use across high-income economies, sourced from the World Bank Databank.

similar results. The main challenge lies in constructing energy price series, especially for clean energy in the early part of the sample. To address this, we make three assumptions. First, all countries face the same energy prices. Second, fossil fuel prices are, as before, proxied by the price of Brent crude oil. Third, the price of green energy is proxied by the median levelized cost across bio-energy, geothermal, offshore wind, solar photovoltaic, concentrated solar power, hydro-power, and onshore wind.[24] The left panel of Figure 13 plots the resulting series, highlighting the decline in green energy prices over the last three decades.

We next source fossil fuel energy use and alternative and nuclear energy use from the World Bank DataBank, taking the median across high-income economies. The center and right panels of Figure 14 show the resulting series, highlighting the expected surge in clean energy use and the inverted-U pattern in fossil fuel consumption. Finally, using gross domestic product from the Maddison Project database, we compute the shares of brown and green energy expenditures in output. In 1990, the first year of our sample, these shares were 4% for brown energy and 2% for green energy. We therefore set $\mu_{f0} = 0.04$ and $\nu_{f0} = 0.02$.

The remaining parameter κ determines the speed of change and it will be jointly calibrated with other parameters (see below).

Elasticity of final output with respect to capital. Because of constant returns to scale, the elasticity of final output with respect to capital, α_f, equals one minus the sum of the elasticities

[24]Source: International Renewable Energy Agency (IRENA), Renewable Power Generation Costs. Not all series are available from 1990 onwards; we take the median of available data.

with respect to labor, brown energy, and green energy. Having calibrated the latter two in the previous subsection, we compute the labor share of GDP across high-income economies to determine α_f.

The Penn World Table (Feenstra et al., 2015) implies that the median labor share of GDP across high-income economies over 1990-2019 was 56%.[25] Combining this figure with the energy shares obtained above yields a capital elasticity of $\alpha_f = 0.38$, which is close to the one-third value commonly assumed in macroeconomic models.

Elasticity of brown energy with respect to fossil fuels. Let $h(t)$ denote carbon intensity, defined as the tons of CO_2 emitted per thousand dollars of output at constant 2011 prices. In our model, this corresponds to

$$h(t) \coloneqq \frac{\epsilon\, x(t)}{y(t)} \;=\; \frac{\epsilon\, \mu_b\, \mu_f(t)}{c_x}\,.$$

where the right expression comes from equilibrium conditions (see Appendix B.4 for details). In 1990, the median $h(0)$ across high-income economies was 0.45. Remembering that $\mu_f(0) = \mu_{f0}$ and using the calibrated values of c_x, ϵ, and μ_{f0}, this implies an elasticity of brown energy with respect to fossil fuels of $\mu_b = 0.78$.

Elasticity of green energy with respect to capital. We set the elasticity of green energy with respect to capital to $\alpha_g = 0.75$, as in Hillebrand and Hillebrand (2019, 2023).

Elasticity of brown energy with respect to capital. Data from the Labor Force Survey, reported by the International Labor Organization, show that across a sample of 19 high-income economies, roughly 1.5% of total employment was allocated to mining, quarrying, and electricity, gas, and water supply in 1990. This implies that 98.5% of total employment was allocated to the production of final output (i.e., not in energy production), that is $n_f(0) = 0.985$. We show in Appendix B.2 that, using equilibrium conditions, we can also derive

$$n_f(0) = \frac{1 - \alpha_f - \mu_{f0} - \nu_{f0}}{1 - \alpha_f - (\alpha_b + \mu_b)\mu_{f0} - \alpha_g \nu_{f0}}\,,$$

which allows us to compute $\alpha_b = 0.13$.

TFP parameters in energy sectors. Parameters θ_b and θ_g scale total factor productivity in the brown and green energy sectors. Our calibration proceeds as follows. Given the TFP parameter in the final goods sector (θ_{f0}, which will be jointly calibrated with other parameters, see below) and the mean initial capital stock $k_{0,\mu}$ (obtained from our kernel-based approximation of the distribution), we choose θ_b and θ_g to match two moments. First, the initial green energy share of total energy use is 5.2%, the median value across high-income countries in 1990. Second, the initial energy-to-output ratio is 5.6×10^6, corresponding to

[25] As before, extending the sample to low- and middle-income economies delivers a similar calibration.

the median value across high-income countries in 1990, expressed in watt-hour per n 2011 U.S. dollars.[26]

We show in Appendix B.5 that finding $\{\theta_b, \theta_g\}$ to match the two targets (denoted as $s_g(0)$ and $r_e(0)$ in Appendix) reduces to solving a linear system of two equations in the two unknowns.

TFP parameters in the final sector. As explained in Section 5.1, to preserve a meaningful cross-sectional distribution, we follow Krueger et al. (2016) and introduce an aggregate-demand externality. In practice, we consider that total factor productivity in sector f is no longer the constant θ_f, but is instead given by (see Section 5.1 for details and properties)

$$\theta_f(t,k) = \theta_{f0}\left(1 + \mathrm{e}^{-\beta_g t}\,\frac{1-\mathrm{e}^{-\beta_f(k-k_{0,\mu})}}{1+\mathrm{e}^{-\beta_f(k-k_{0,\mu})}}\right).$$

Therefore, the three parameters $\{\theta_{f0}, \beta_f, \beta_g\}$ of this function need to be calibrated, along with the parameter κ from the logistic function $\mu_f(t)$ (see above). Because solving our MFG system is numerically costly, we cannot rely on a full estimation procedure. Instead, we construct a discrete, course grid for these four parameters and evaluate the model at each point on that grid. For every parameter combination, we compare the model's implications with four empirical targets: (i) a renewable-energy share of 10% in 2021; (ii) an 18% increase in atmospheric CO_2 between 1990 and 2021; (iii) a 130% rise in median capital per capita between 1990 and 2019; and (iv) a 30% decline in the coefficient of variation of capital per capita over the same period. The first target matches the average value in high-income economies in 2021; the second matches the observed rise in atmospheric CO_2; and the last two correspond to changes in the capital distribution across our sample of 134 countries.

The grid search yields: $\kappa = 0.8$, $\theta_{f0} = 0.73$, $\beta_f = 15$, and $\beta_g = 0.2$. Under these values, the model produces a renewable-energy share of 11% in 2021, an increase in atmospheric CO_2 of 23%, an 80% rise in median capital per capita between 1990 and 2019, and a 30% decline in the coefficient of variation over the same period. The model does not match the four targets exactly, which is expected given the coarseness of the grid. Still, the implied statistics fall within plausible ranges.

Appendix B. Equilibrium Conditions

In general, any lowercase variable $z(t)$ denotes the detrended counterpart of its non-detrended form $Z(t)$, defined as $z(t) \coloneqq Z(t)/(A(t)N(t))$. Assumption 2 defines the evolution of $A(t)$ and $N(t)$. Equations refer to an individual country i but, to avoid overloaded notations, we do not explicitly index variable by i.

[26] Energy data come from the World Bank DataBank, and GDP data from the Maddison Project Database.

B.1. **Production sectors and fossil fuel extraction.** In the final goods sector, a representative firm maximizes

$$Y(t) - r(t)K_f(t) - p_b(t)E_b(t) - p_g(t)E_g(t) - w(t)N_f(t)\,,$$

with $Y(t) = \theta_f K_f(t)^{\alpha_f} E_b(t)^{\mu_f} E_g(t)^{\nu_f} N_f(t)^{1-\alpha_f-\mu_f-\nu_f}$. After detrending, the problem writes

$$y(t) - r(t)k_f(t) - p_b(t)e_b(t) - p_g(t)e_g(t) - w(t)n_f(t)\,,$$

with $y(t) = \theta_f k_f(t)^{\alpha_f} e_b(t)^{\mu_f} e_g(t)^{\nu_f} n_f(t)^{1-\alpha_f-\mu_f-\nu_f}$, which gives the four FOC's

$$\begin{aligned} r(t) &= \alpha_f y(t)/k_f(t)\,,\\ p_b(t) &= \mu_f y(t)/e_b(t)\,,\\ p_g(t) &= \nu_f y(t)/e_g(t)\,,\\ w(t) &= (1-\alpha_f-\mu_f-\nu_f)y(t)/n_f(t)\,. \end{aligned}$$

In the brown energy sector, a representative firm maximizes

$$p_b(t)E_b(t) - r(t)K_b(t) - v(t)X(t) - w(t)N_b(t)\,,$$

with $E_b(t) = \theta_b K_b(t)^{\alpha_b} X(t)^{\mu_b} N_b(t)^{1-\alpha_b-\mu_b}$. After detrending, the problem gives the three FOC's

$$\begin{aligned} r(t) &= \alpha_b p_b(t)e_b(t)/k_b(t)\,,\\ v(t) &= \mu_b p_b(t)e_b(t)/x(t)\,,\\ w(t) &= (1-\alpha_b-\mu_b)p_b(t)e_b(t)/n_b(t)\,. \end{aligned}$$

In the green energy sector, a representative firm maximizes

$$p_g(t)E_g(t) - r(t)K_g(t) - w(t)N_g(t)\,,$$

with $E_g(t) = \theta_g K_g(t)^{\alpha_g} N_g(t)^{1-\alpha_g}$. After detrending, the problem gives the two FOC's

$$\begin{aligned} r(t) &= \alpha_g p_g(t)e_g(t)/k_g(t)\,,\\ w(t) &= (1-\alpha_g)p_g(t)e_g(t)/n_g(t)\,. \end{aligned}$$

We denote $\bar{X}_t$ as the aggregate (across all countries) fossil fuel demand. There is a single country extracting and selling $\bar{X}_t$. In this country, a representative firm maximizes

$$v(t)\bar{X}_t - c_x\bar{X}_t\,.$$

After detrending, the problem gives the FOC: $v(t) = c_x$.

B.2. **Aggregation across sectors.** In each country, we have $A(t)N(t) = N_f(t) + N_b(t) + N_g(t)$ or, after detrending, $1 = n_f(t) + n_b(t) + n_g(t)$. Because the wage $w(t)$ is the same across sector, we obtain from the three labor FOCs

$$\frac{n_f(t)}{1-\alpha_f-\mu_f-\nu_f} = \frac{n_b(t)}{\mu_f(1-\alpha_b-\mu_b)} = \frac{n_g(t)}{\nu_f(1-\alpha_g)}\,.$$

Plugging these expressions in the aggregate equation finally gives

$$\begin{aligned} n_f(t) &= (1-\alpha_f-\mu_f-\nu_f)/(\mu-\alpha)\,,\\ n_b(t) &= \mu_f(1-\alpha_b-\mu_b)/(\mu-\alpha)\,,\\ n_g(t) &= \nu_f(1-\alpha_g)/(\mu-\alpha)\,. \end{aligned}$$

with α and μ from Definition 1. Similarly, in each country, we have $K(t) = K_f(t) + K_b(t) + K_g(t)$ or, after detrending, $k(t) = k_f(t) + k_b(t) + k_g(t)$. Because the interest rate $r(t)$ is the same across sector, we obtain from the three capital FOCs

$$\frac{k_f(t)}{\alpha_f} = \frac{k_b(t)}{\mu_f\alpha_b} = \frac{k_g(t)}{\nu_f\alpha_g}\,.$$

Plugging these expressions in the aggregate equation finally gives

$$\begin{aligned} k_f(t) &= (\alpha_f/\alpha)k(t)\,,\\ k_b(t) &= (\mu_f\alpha_b/\alpha)k(t)\,,\\ k_g(t) &= (\nu_f\alpha_g/\alpha)k(t)\,. \end{aligned}$$

Combining the FOCs with respect to brown energy (final goods sector) and fossil fuels (brown energy sector) gives

$$\frac{x(t)}{y(t)} = \frac{\mu_f\mu_b}{c_x}\,.$$

Finally, plugging the brown energy and green energy productions functions into the final goods production functions, and using the above expressions for $n_f(t)$, $n_b(t)$, $n_g(t)$, $k_f(t)$, $k_b(t)$, $k_g(t)$ and $x(t)$ give

$$\begin{aligned} &y(t) = \theta_f\theta_b^{\mu_f}\theta_g^{\nu_t}k_f(t)^{\alpha_f}k_b(t)^{\mu_f\alpha_b}k_g(t)^{\nu_f\alpha_g}n_f(t)^{1-\alpha_f-\mu_f-\nu_f}n_b(t)^{\mu_f(1-\alpha_b-\mu_b)}n_g(t)^{\nu_f(1-\alpha_g)}x(t)^{\mu_f\mu_b}\,,\\ \Leftrightarrow\ &y(t) = \tilde{\theta}\tilde{k}k(t)^{\alpha}\tilde{n}\tilde{x}y(t)^{\mu_f\mu_b}\,,\\ \Leftrightarrow\ &y(t)^{\mu} = \tilde{\theta}\tilde{k}\tilde{n}\tilde{x}k(t)^{\alpha}\,,\\ \Leftrightarrow\ &y(t) = \tilde{y}k(t)^{\alpha/\mu}\,, \end{aligned}$$

where we make use of Definition 1.

B.3. **Household.** In each country, a representative household maximizes

$$\int_0^\infty \mathrm{e}^{-\rho t}\,\frac{C(t)^{1-\sigma}-1}{1-\sigma}\,\mathrm{d}t\,,$$

under $\dot{K}(t) = w(t)A(t)N(t) + (r(t)-\delta)K(t) - C(t)$. The Hamiltonian writes

$$H(t) = \mathrm{e}^{-\rho t}\,\frac{C(t)^{1-\sigma}-1}{1-\sigma} + \lambda(t)(w(t)A(t)N(t) + (r(t)-\delta)K(t) - C(t))\,,$$

and the necessary conditions are $\partial H(t)/\partial C(t) = 0$, $\partial H(t)/\partial K(t) = -\dot{\lambda}(t)$ and $\partial H(t)/\partial \lambda(t) = \dot{K}(t)$. After detrending and using Assumption 2, the necessary conditions becomes

$$\begin{aligned}\dot{k}(t) &= w(t) + (r(t) - (\delta + p(t)))k(t) - c(t)\,,\\ \frac{\dot{c}(t)}{c(t)} &= \frac{r(t)-(\delta+\rho)}{\sigma} - p(t)\,.\end{aligned}$$

Combining the capital FOC in the final goods sector, and final expressions for $k_f(t)$ and $y(t)$, we have

$$r(t) = \alpha_f \frac{y(t)}{k_f(t)} = \alpha\frac{y(t)}{k(t)} = \alpha\tilde{y}k(t)^{\frac{\alpha}{\mu}-1}\,.$$

Similarly, combining the labor FOC in the final goods sector, and final expressions for $n_f(t)$ and $y(t)$, we have

$$w(t) = (\mu-\alpha)\tilde{y}k(t)^{\frac{\alpha}{\mu}}\,.$$

Injecting the expressions for $r(t)$ and $w(t)$ into the necessary conditions yields the first two equations in Proposition 1. The initial capital stock $K(0)$ is given and we define $k_0 \coloneqq k(0) = K(0)/(A(0)N(0))$, where we normalize $A(0)$ and $N(0)$ to 1. The transversality condition is

$$\lim_{t\to\infty} \lambda(t)K(t) = 0\,.$$

Note that

$$\lambda(t)K(t) = \mathrm{e}^{-\rho t}\,C(t)^{-\sigma}K(t) = \mathrm{e}^{-\left(\rho t - (1-\sigma)\int_0^t p(u)\mathrm{d}t\right)}\,c(t)^{-\sigma}k(t)\,.$$

This gives the initial condition on $k(t)$ and the transversality condition in Proposition 1.

B.4. **Climate determinants.** The climate bloc is common to all countries. Atmospheric CO_2 evolves as

$$\dot{S}(t) = \epsilon\bar{X}(t) - \psi S(t)\,,$$

which gives $\dot{s}(t) = \epsilon\bar{x}(t) - (\psi + p(t))S(t)$, after detrending. From our above computations, we know that in each country,

$$x(t) = \frac{\mu_f\mu_b}{c_x}y(t) = \frac{\mu_f\mu_b}{c_x}\tilde{y}k(t)^{\alpha/\mu}\,.$$

Therefore, aggregate emissions are

$$\epsilon\bar{x}_t = \int_0^\infty \epsilon\frac{\mu_f\mu_b}{c_x}\tilde{y}k(t)^{\alpha/\mu}u(t,k)\mathrm{d}k = \int_0^\infty \phi\tilde{y}k(t)^{\alpha/\mu}u(t,k)\mathrm{d}k\,,$$

using Assumption 1 and Definition 1. This gives the third equation in Proposition 1, with $s_0 \coloneqq s(0) = S(0)/(A(0)N(0)) = S(0)$. Finally growth evolves as

$$p(t) = -\gamma \frac{\dot{S}(t)}{S(t)} = -\gamma \left(\epsilon \frac{\bar{X}(t)}{S_t} - \psi \right) = -\gamma \left(\epsilon \frac{\bar{x}(t)}{s_t} - \psi \right) .$$

Using the above expression for $\epsilon \bar{x}(t)$ yields the last equation in Proposition 1, with $p_0 \coloneqq p(0)$ given.

B.5. **Variables of interest.** The production functions for energies are

$$\begin{aligned} e_b(t) &= \theta_b k_b(t)^{\alpha_b} \, x(t)^{\mu_b} \, n_b(t)^{1-\alpha_b-\mu_b} \, , \\ e_g(t) &= \theta_g k_g(t)^{\alpha_g} \, n_g(t)^{1-\alpha_g} \, . \end{aligned}$$

We know from Appendix B.2 that

$$\begin{aligned} n_b(t) &= \mu_f(1-\alpha_b-\mu_b)/(\mu-\alpha) \, , \\ n_g(t) &= \nu_f(1-\alpha_g)/(\mu-\alpha) \, , \\ k_b(t) &= (\mu_f \alpha_b/\alpha) k(t) \, , \\ k_g(t) &= (\nu_f \alpha_g/\alpha) k(t) \, , \end{aligned}$$

and from Appendix B.4 that

$$x(t) = \frac{\mu_f \mu_b}{c_x} \tilde{y} k(t)^{\alpha/\mu} \, .$$

Finally, Definition 1 shows that α and μ only depend on the elasticities $\mathcal{E} = \{\alpha_f, \alpha_b, \alpha_g, \mu_f, \mu_b, \nu_g\}$, and that $\tilde{y}$ only depends on $\mathcal{E}$, θ_f, θ_b and θ_g. Therefore, we can write

$$\begin{aligned} e_b(t) &= G_b(\theta_f, \theta_b, \theta_g, \mathcal{E}, k(t)) \, , \\ e_g(t) &= G_g(\theta_g, \mathcal{E}, k(t)) \, , \end{aligned}$$

where $G_b(\cdot)$ and $G_g(\cdot)$ are functions which can be derived from above. We define the share of green energy to total energy as

$$s_g(t) \coloneqq \frac{e_g(t)}{e_g(t)+e_b(t)} = S_g(\theta_f, \theta_b, \theta_g, \mathcal{E}, k(t)) \, ,$$

where $S_b(\cdot)$ is also a function which can be easily derived. Finally, remembering that $y(t) = \tilde{y} k(t)^{\alpha/\mu}$ from Appendix B.2, we define the energy-to-output ratio as

$$r_e(t) \coloneqq \frac{e_g(t)+e_b(t)}{y(t)} = R_e(\theta_f, \theta_b, \theta_g, \mathcal{E}, k(t)) \, ,$$

where $R_e(\cdot)$ is a function we can derive analytically. Note that at time $t = 0$, for a country with the mean initial capital stock $k_{0,\mu}$, we have

$$\begin{aligned} s_g(0) &= S_g(\theta_{f0}, \theta_b, \theta_g, \mathcal{E}, k_{0,\mu}) \, , \\ r_e(0) &= R_e(\theta_{f0}, \theta_b, \theta_g, \mathcal{E}, k_{0,\mu}) \, . \end{aligned}$$

B.6. **Asymptotic stability.** We compute the Jacobian $\mathcal{J}$ of the system of ODEs in Proposition 1, at the unique interior steady state given in Proposition 2. This yields

$$\mathcal{J} = \begin{pmatrix} \rho & -1 & 0 & -k^* \\ J_k^c & 0 & 0 & J_p^c \\ J_k^s & 0 & -\psi & J_p^s \\ J_k^p & 0 & J_s^p & 0 \end{pmatrix},$$

with

$$\begin{aligned} J_k^c &= -\frac{(\mu-\alpha)(\rho+\delta)}{\sigma\mu}\left(\frac{\mu(\rho+\delta)}{\alpha}-\delta\right), \\ J_p^c &= -\left(\frac{\mu(\rho+\delta)}{\alpha}-\delta\right)\frac{k^*}{\sigma}, \\ J_k^s &= \frac{\phi(\rho+\delta)}{\mu}, \\ J_p^s &= -\frac{\phi(\rho+\delta)}{\alpha\psi}k^*, \\ J_k^p &= -\frac{\alpha\gamma\psi}{\mu k^*}, \\ J_s^p &= \frac{\alpha\gamma\psi^2}{\phi(\rho+\delta)k^*}. \end{aligned}$$

The determinant of the Jacobian is

$$|\mathcal{J}| = -\frac{\gamma\psi}{\sigma\mu}(\mu-\alpha)(\rho+\delta)\left(\frac{\mu(\rho+\delta)}{\alpha}-\delta\right) < 0,$$

meaning that one or three eigenvalues are negative. Given that our model has three state variables and one control variable, we either have a source solution (first case) or a stable solution (second case).

B.7. **Asymptotic stability in a Solow version.** In the Solow version, we remove the second equation in Proposition 1 and replace the first one with

$$\dot{k}(t) = s_r\,\mu\,\tilde{y}\,k(t)^{\frac{\alpha}{\mu}} - (p(t)+\delta)k(t),$$

where $s_r \in (0,1)$ is the exogenous saving rate. The asymptotic steady states are

$$\begin{aligned} k^* &= \left(\frac{s_r\mu\,\tilde{y}}{\delta}\right)^{\frac{\mu}{\mu-\alpha}}, \\ s^* &= \frac{\phi\,\delta}{\psi\mu s_r}k^*, \end{aligned}$$

and the Jacobian is

$$\mathcal{J} = \begin{pmatrix} -\frac{\delta(\mu-\alpha)}{\mu} & 0 & -k^* \\ J_k^s & -\psi & J_p^s \\ J_k^p & J_s^p & 0 \end{pmatrix},$$

with

$$\begin{aligned} J_k^s &= \frac{\alpha\phi\,\delta}{s_r\mu^2}\,, \\ J_p^s &= -\frac{\phi\,\delta}{\psi\mu s_r}k^*\,, \\ J_k^p &= -\frac{\alpha\gamma\psi}{\mu k^*}\,, \\ J_s^p &= \frac{s_r\mu\gamma\psi^2}{\phi\,\delta k^*}\,. \end{aligned}$$

The determinant of the Jacobian is

$$|\mathcal{J}| = -\gamma\psi\delta\left(\frac{\mu-\alpha}{\mu}\right) < 0\,,$$

meaning that one or three eigenvalues are negative. Given that our model has three state variables, we either have a source solution (first case) or a stable solution (second case). We can compute the characteristic polynomial $\mathcal{P}(\lambda) = a_3\lambda^3 + a_2\lambda^2 + a_1\lambda + a_0$ of the matrix $\mathcal{J}$ and we obtain

$$\begin{aligned} a_0 &= \gamma\psi\delta\left(\frac{\mu-\alpha}{\mu}\right) > 0\,, \\ a_1 &= \psi(\delta+\gamma)\left(\frac{\mu-\alpha}{\mu}\right) > 0\,, \\ a_2 &= \psi + \delta\left(\frac{\mu-\alpha}{\mu}\right) > 0\,, \\ a_3 &= 1\,. \end{aligned}$$

We then apply the Routh–Hurwitz theorem (see Bodson, 2020, for details) stating that the polynomial $\mathcal{P}(\lambda)$ has three negative roots if and only if all $a_i > 0$ and $a_2a_1 - a_3a_0 > 0$. The first condition is straightforward. The second condition writes

$$\left(\psi + \delta\left(\frac{\mu-\alpha}{\mu}\right)\right)(\gamma+\delta) > \gamma\delta\,.$$

We observe that this condition is only violated under extreme calibrations, for instance if $\alpha/\mu \to 1$ (AK technology), $\psi \to 0$ (all emissions remain permanently in the atmosphere), and γ and δ very large.

Appendix C. Backward-forward MFG system

C.1. **HJB equation.** We define

$$\begin{aligned} v(t,k(t)) &= \max_{c(s)} \int_t^\infty \mathrm{e}^{-\rho(s-t)}\,\mathcal{U}(C(s))\,\mathrm{d}s\,, \\ &= \max_{c(s)} \int_t^{t+\mathrm{d}t} \mathrm{e}^{-\rho(s-t)}\,\mathcal{U}(C(s))\,\mathrm{d}s + \int_{t+\mathrm{d}t}^\infty \mathrm{e}^{-\rho t}\,\mathrm{e}^{-\rho(s-(t+\mathrm{d}t))}\,\mathcal{U}(C(s))\,\mathrm{d}s\,, \\ &= \max_{c(s)} \int_t^{t+\mathrm{d}t} \mathrm{e}^{-\rho(s-t)}\,\mathcal{U}(C(s))\,\mathrm{d}s + \mathrm{e}^{-\rho t}\,v(t+\mathrm{d}t,k(t+\mathrm{d}t))\,. \end{aligned}$$

We consider the following first order approximations

$$\begin{aligned} \int_t^{t+\mathrm{d}t} \mathrm{e}^{-\rho(s-t)}\,\mathcal{U}(C(s))\,\mathrm{d}s &\approx \mathcal{U}(C(t))\,\mathrm{d}t\,, \\ \mathrm{e}^{-\rho t} &\approx 1-\rho\,\mathrm{d}t\,, \\ v(t+\mathrm{d}t,k(t+\mathrm{d}t)) &\approx v(t,k(t)) + \frac{\partial v}{\partial t}(t,k(t))\mathrm{d}t + \frac{\partial v}{\partial k}(t,k(t))\dot{k}(t)\mathrm{d}t\,, \end{aligned}$$

and we obtain

$$\rho\,v(t,k(t)) = \max_{c(t)} \mathcal{U}(C(t)) + (1-\rho\,\mathrm{d}t)\left(\frac{\partial v}{\partial t}(t,k(t)) + \frac{\partial v}{\partial k}(t,k(t))\dot{k}(t)\right)\,.$$

Assuming that $\mathrm{d}t \to 0$, taking our utility function with $C(t) = A(t)N(t)c(t)$ and the law of motion for $k(t)$ from Proposition 1, we finally obtain the HJB equation (3) in Proposition 3.

When $k = 0$, there is no production and therefore no consumption. If $\sigma \geq 1$, then $\mathcal{U}(C) = -\infty$ when $C \to 0$ and hence $v(t,0) = -\infty$. If $\sigma < 1$, then $\mathcal{U}(0) = -1/(1-\sigma)$ and $v(t,0) = -\int_t^\infty \mathrm{e}^{-\rho(s-t)}/(1-\sigma)\,\mathrm{d}s = -1/(\rho(1-\sigma))$. We moreover have that $\mathcal{U}'(C) = +\infty$ when $C \to 0$, which gives $\partial v/\partial k(t,0) = +\infty$. These are our Cauchy boundary conditions.

Finally, maximizing the right-hand side of the HJB equation gives

$$\mathrm{e}^{(1-\sigma)\int_0^t p(u)\mathrm{d}u}\,c^{-\sigma} = \frac{\partial v}{\partial k}(t,k(t))\,.$$

Plugging this into the transversality condition in Proposition 1 gives the terminal condition for the HJB problem.

C.2. **Transport equation.** We know $\dot{k} = i(t,k)$, with $(t,k) \in \mathbb{R}^+ \times \mathbb{R}^+$. We define $u(t,k)$ as the density function of k, with initial condition $u(0,k) = u_0(k) \geq 0$ and $\int_0^\infty u_0(k)\mathrm{d}k = 1$ (Definition 1). We moreover impose $u(t,0) = 0$ and $\lim_{k\to\infty} u(t,k) = 0$ (Dirichlet boundary conditions). We have to show that

$$\frac{\partial}{\partial t}u(t,k) + \frac{\partial}{\partial k}\left(i(t,k)u(t,k)\right) = 0\,.$$

To do so, let us take any function $f(t,k) : \mathbb{R}^+ \times \mathbb{R}^+ \longmapsto \mathbb{R}$ which is $\mathcal{C}^1$ in both arguments. Then

$$\begin{aligned}\mathrm{d}f(t,k) &= \frac{\partial f(t,k)}{\partial t}\,\mathrm{d}t + \frac{\partial f(t,k)}{\partial k}\,\mathrm{d}k \\ &= \frac{\partial f(t,k)}{\partial t}\,\mathrm{d}t + \frac{\partial f(t,k)}{\partial k}\,i(t,k)\,\mathrm{d}t \\ &= \left(\frac{\partial f(t,k)}{\partial t} + \frac{\partial f(t,k)}{\partial k}\,i(t,k)\right)\,\mathrm{d}t\,.\end{aligned}$$

Taking expectations on all k gives

$$\begin{aligned}\frac{\mathbb{E}_k\,\mathrm{d}f(t,k)}{\mathrm{d}t} &= \mathbb{E}_k\,\frac{\partial f(t,k)}{\partial t} + \mathbb{E}_k\,\frac{\partial f(t,k)}{\partial k}\,i(t,k) \\ &= \int_0^\infty \frac{\partial f(t,k)}{\partial t}\,u(t,k)\,\mathrm{d}k + \int_0^\infty \frac{\partial f(t,k)}{\partial k}\,i(t,k)\,u(t,k)\,\mathrm{d}k\,.\end{aligned}$$

Moreover, we have

$$\begin{aligned}\frac{\mathbb{E}_k\,\mathrm{d}f(t,k)}{\mathrm{d}t} &= \frac{\mathrm{d}\,\mathbb{E}_k\,f(t,k)}{\mathrm{d}t} = \frac{\mathrm{d}}{\mathrm{d}t}\int_0^\infty f(t,k)\,u(t,k)\,\mathrm{d}k \\ &= \int_0^\infty \frac{\mathrm{d}}{\mathrm{d}t}\left(f(t,k)\,u(t,k)\right)\,\mathrm{d}k \\ &= \int_0^\infty \frac{\partial f(t,k)}{\partial t}\,u(t,k)\,\mathrm{d}k + \int_0^\infty f(t,k)\,\frac{\partial u(t,k)}{\partial t}\,\mathrm{d}k\,.\end{aligned}$$

By equating the two above expressions, we obtain

$$\int_0^\infty \frac{\partial f(t,k)}{\partial k}\,i(t,k)\,u(t,k)\,\mathrm{d}k = \int_0^\infty f(t,k)\,\frac{\partial u(t,k)}{\partial t}\,\mathrm{d}k\,.$$

Integrating by part the left-hand side, and using the Dirichlet boundary conditions, gives

$$-\int_0^\infty f(t,k)\,\frac{\partial}{\partial k}\left(i(t,k)\,u(t,k)\right)\,\mathrm{d}k = \int_0^\infty f(t,k)\,\frac{\partial u(t,k)}{\partial t}\,\mathrm{d}k\,.$$

Since this equation must hold for any function $f(t,k)$, we get

$$-\frac{\partial}{\partial k}\left(i(t,k)\,u(t,k)\right) = \frac{\partial u(t,k)}{\partial t}\,.$$

C.3. **Density.** $u(t,k)$ is the probability density function of detrended capital k at time t, and evolves according to the transport equation (4). Let us assume any other variable z, which is a function of k according to $z = f(k)$. We moreover assume that the function $f(\cdot)$ is bijective such that $f^{-1}(\cdot)$ exists. We define $u_z(t,z)$ as the probability density function of the variable z at time t. This density is given by

$$u_z(t,z) = u\left(t, f^{-1}(z)\right)\left|\frac{\partial f^{-1}(z)}{\partial z}\right|\,.$$

FIGURE 15. Accuracy tests

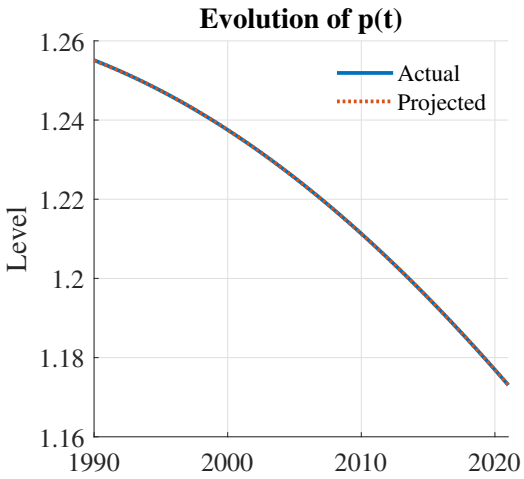

Residual type in HJB	Value
Mean	-2.1×10^{-4}
Median	-2.7×10^{-4}
Mean absolute	1.0×10^{-2}
Median absolute	1.4×10^{-3}
Max absolute	1.3×10^{-0}
Mean relative absolute	1.7×10^{-3}
Median relative absolute	1.8×10^{-4}
Max relative absolute	2.8×10^{-1}

Notes. The left panel shows the actual dynamics of $p(t)$ alongside the dynamics projected by individual countries using $f(\cdot)$. The right panel reports HJB residuals evaluated on the fine transport grid, including absolute and relative absolute measures.

APPENDIX D. NUMERICAL METHODS

This section evaluates the accuracy of the numerical solution over the validation period 1990–2021. As described in the main text, we solve the model on the domain $[t_\ell, t_h] \times [k_\ell, k_h]$. Since one model period corresponds to 32 years, we set $t_\ell = 0$ and $t_h = 1$. For capital, we choose $k_\ell = 5 \times 10^{-4}$ and $k_h = 0.3$, which span the full support of the empirical distribution of $k(0)$ constructed from the data (see Appendix A.2). Section 4 explains that solving the transport equation requires a finer grid than solving the HJB equation. Accordingly, we use 600 grid points in the capital dimension and 1,200 in the time dimension for the transport equation, ensuring that the Courant–Friedrichs–Lewy condition holds at every grid point during the finite difference scheme. In contrast, the HJB equation is solved on a coarser grid with 50 points in capital and 7 in time. To evaluate the HJB solution on the transport grid, we apply cubic interpolation.

Regarding the fixed-point algorithm (see equation 6), we specify the function $f(t \mid \boldsymbol{\Theta})$ as

$$p(t) = \exp\left(\theta_0 + \theta_1 t + \theta_2 t^2\right),$$

and estimate the parameters $\boldsymbol{\Theta}$ by constrained OLS within the algorithm described in the main text. The constraint $\theta_2 < 0$ ensures that $p(t) \to 0$ as $t \to \infty$.

Together with the descriptions in the main text, these observations document the solution method. All MATLAB code is available upon request.

We now assess the accuracy of the solution method. Focusing first on the HJB equation, the main text defines the approximating residual at grid point (t, k) as $R(t, k) = \mathcal{H}[\hat{v}(t, k)]$. We evaluate $R(t, k)$ on the fine grid used to solve the transport equation. In addition, we consider its absolute value, $|R(t, k)|$, and its relative absolute value, $|R(t, k)/\hat{v}(t, k)|$. The right panel of Figure 15 reports the results. Overall, the residuals are small. Both the mean and median residuals are close to zero, and the absolute residuals have a mean of order 10^{-2} and a median of order 10^{-3}. Relative absolute residuals are also small, indicating that the numerical solution of the HJB equation is accurate over most of the state space. The largest residuals arise at extremely low values of k. However, this region of the state space carries essentially zero probability mass under the density generated by the transport equation and is therefore does not affect the results.

Turning to the transport equation, we assess its accuracy by monitoring the total probability mass, $M(t) = \int_{k_l}^{k_h} u(t, k)\, dk$, over the simulation period. Across the 1,200 time nodes, the total mass remains very close to one, reaching 0.999 at node 600 and 1.003 at node 1,200. The approximated solution is therefore highly accurate, consistent with the well-known reliability of the upwind finite difference scheme over relatively short time horizons.

Lastly, the left panel of Figure 15 compares the actual path of $p(t)$ with the path projected by individual countries using $f(t \mid \boldsymbol{\Theta})$. The two series overlap, indicating that agents' perceived dynamics align closely with the realized evolution of $p(t)$.

Appendix E. Global carbon tax

E.1. **Carbon tax with domestic redistribution.** In each country, we introduce a carbon tax which is redistributed lump sum to the household

$$m(t) = \tau c_x\, x(t)\,,$$

where $\tau \geq 0$ is the carbon tax rate and $m(t)$ is the lump-sum transfer. The carbon tax changes the FOC with respect to fossil fuels as

$$x(t) = \frac{\mu_f \nu_b}{(1+\tau)\, c_x}\, y(t)\,.$$

This modifies the definition of aggregate parameters

$$\phi := \epsilon \, \frac{\mu_f \mu_b}{(1+\tau)\, c_x} > 0\,,$$
$$\tilde{x} := \left(\frac{\mu_f \mu_b}{(1+\tau)\, c_x} \right)^{\mu_f \mu_b} > 0\,.$$

Using the new FOC, the budget constraint becomes

$$m(t) = \tau c_x \, x(t) = \frac{\tau}{1+\tau} \, (1-\mu) \, \tilde{y} k(t)^{\frac{\alpha}{\mu}}\,,$$

and the evolution of capital is

$$\begin{aligned} \dot{k}(t) &= \mu \, \tilde{y} \, k(t)^{\frac{\alpha}{\mu}} - (p(t)+\delta) k(t) - c(t) + m(t)\,, \\ &= \left(\mu + \frac{\tau}{1+\tau} \, (1-\mu) \right) \, \tilde{y} \, k(t)^{\frac{\alpha}{\mu}} - (p(t)+\delta) k(t) - c(t)\,. \end{aligned}$$

E.2. **Consumption equivalent measure.** We consider a truncated value function, i.e. we compute the discounted utility only up to a time horizon $T \geq 0$. At any initial time t_0 and at a given capital level k, the trucated value functions in the baseline $v_T^{bas}(t_0, k)$ and under a carbon tax policy $v_T^{tax}(t_0, k)$ are

$$\begin{aligned} v_T^{bas}(t_0,k) &= \int_{t_0}^{t_0+T} \mathrm{e}^{-\rho(t-t_0)} \, \frac{\left(C^{bas}(t)\right)^{1-\sigma} - 1}{1-\sigma} \, \mathrm{d}t\,, \\ v_T^{tax}(t_0,k) &= \int_{t_0}^{t_0+T} \mathrm{e}^{-\rho(t-t_0)} \, \frac{\left(C^{tax}(t)\right)^{1-\sigma} - 1}{1-\sigma} \, \mathrm{d}t \\ &= \int_{t_0}^{t_0+T} \mathrm{e}^{-\rho(t-t_0)} \, \frac{\left((1+\varphi_T(t_0,k)) C^{bas}(t)\right)^{1-\sigma} - 1}{1-\sigma} \, \mathrm{d}t\,, \end{aligned}$$

where $\varphi_T(t_0, k)$ denotes the corresponding consumption equivalent measure. With a log utility, we obtain

$$v_T^{tax}(t_0,k) - v_T^{bas}(t_0,k) = \mathrm{e}^{\rho t_0} \ln(1+\varphi_T(t_0,k)) \int_{t_0}^{t_0+T} \mathrm{e}^{-\rho t} \, \mathrm{d}t = \ln(1+\varphi_T(t_0,k)) \frac{1-\mathrm{e}^{-\rho T}}{\rho}\,,$$

which gives

$$\varphi_T(t_0,k) = \mathrm{e}^{\frac{\rho\left(v_T^{tax}(t_0,k) - v_T^{bas}(t_0,k)\right)}{1-\mathrm{e}^{-\rho T}}} - 1\,.$$

E.3. **Carbon tax with cross-country redistribution.** We here describe how we solve the model under a global carbon tax with uniform redistribution across countries.[27] The carbon tax modifies the FOC with respect to fossil fuels as well as the definitions of ϕ and

[27] The same approach applies to the model with an international capital market; we omit the details for brevity.

$\tilde{x}$ as in Appendix E.1. However, under international redistribution, *total* receipts from the tax must be equal to *total* transfers

$$m(t) = \tau \, c_x \, \mu_x(t) \,,$$

where $\mu_x(t)$ is the cross-sectional average of fossil fuel use at time t. Once again, we use a fixed-point algorithm and specify

$$m(t) = f_m(t \mid \boldsymbol{\Theta_m}) \,.$$

We estimate the parameters $\boldsymbol{\Theta_m}$ by constrained OLS within the algorithm described in the main text, and assume

$$f_m(t \mid \boldsymbol{\Theta_m}) = \exp(\omega_0 + \omega_1 t) \,,$$

where we impose $\omega_1 < 0$ to ensure that $m(t) \to 0$ as $t \to \infty$. This specification performs well, delivering an absolute median error of 4.6×10^{-5} over the period 2021–2050. The corresponding absolute maximal error is 1.4×10^{-4}.

Using this expression for $m(t)$, the evolution of capital is

$$\dot{k}(t) = \mu \, \tilde{y} \, k(t)^{\frac{\alpha}{\mu}} - (p(t) + \delta) k(t) - c(t) + m(t) \,.$$

E.4. **Carbon tax with green capital subsidy.** In each country, we introduce a carbon tax which is redistributed through firm subsidies to green capital

$$\tilde{\tau}(t) \, r(t) k_g(t) = \tau c_x \, x(t) \,,$$

where $\tau \geq 0$ is the carbon tax rate and $\tilde{\tau}(t)$ is the green capital subsidy rate. This modifies the FOC with respect to fossil fuels as well as the definitions of ϕ and $\tilde{x}$ as in Appendix E.1. Moreover, the carbon tax changes the FOC with respect to green capital, which implies

$$\begin{aligned}
k_f(t) &= \frac{\alpha_f (1 - \tilde{\tau}(t))}{\alpha - \tilde{\tau}(t)(\alpha_f + \mu_f \alpha_b)} \, k(t) \,, \\
k_b(t) &= \frac{\mu_f \alpha_b (1 - \tilde{\tau}(t))}{\alpha - \tilde{\tau}(t)(\alpha_f + \mu_f \alpha_b)} \, k(t) \,, \\
k_g(t) &= \frac{\nu_f \alpha_g}{\alpha - \tilde{\tau}(t)(\alpha_f + \mu_f \alpha_b)} \, k(t) \,.
\end{aligned}$$

This also modifies the definition of the aggregate parameter

$$\tilde{k} \coloneqq \frac{\alpha_f^{\alpha_f} (\mu_f \alpha_b)^{\mu_f \alpha_b} (\nu_f \alpha_g)^{\nu_f \alpha_g}}{(\alpha - \tilde{\tau}(t)(\alpha_f + \mu_f \alpha_b))^{\alpha}} \, (1 - \tilde{\tau}(t))^{\alpha_f + \mu_f \alpha_b} \,.$$

Note that

$$r(t) = \alpha_f \frac{y(t)}{k_f(t)} = \frac{\alpha - \tilde{\tau}(t)(\alpha_f + \mu_f \alpha_b)}{1 - \tilde{\tau}(t)} \, \tilde{y} k(t)^{\frac{\alpha}{\mu} - 1} \,.$$

Using this expression, as well as the new FOCs for $x(t)$ and $k_g(t)$, the budget constraint becomes

$$\begin{aligned} \tilde{\tau}(t)\, r(t) k_g(t) &= \tau c_x\, x(t) \\ \Leftrightarrow\ \frac{\tilde{\tau}(t)}{1-\tilde{\tau}(t)}\, \nu_f \alpha_g &= \frac{\tau}{1+\tau}\, \mu_f \mu_b\,. \end{aligned}$$

Because the parameter μ_f is time-varying and tends to 0 when $t \to \infty$, the subsidy rate $\tilde{\tau}(t)$ vanishes asymptotically. The evolution of capital and consumption is given by

$$\begin{aligned} \dot{k}(t) &= \left(\mu + \frac{\tau}{1+\tau}\,(1-\mu)\right) \tilde{y}\, k(t)^{\frac{\alpha}{\mu}} - (p(t)+\delta)k(t) - c(t)\,, \\ \frac{\dot{c}(t)}{c(t)} &= \frac{\frac{\alpha - \tilde{\tau}(t)(\alpha_f + \mu_f \alpha_b)}{1-\tilde{\tau}(t)}\, \tilde{y}\, k(t)^{\frac{\alpha}{\mu}-1} - (\rho+\delta)}{\sigma} - p(t)\,. \end{aligned}$$

We observe that a green capital subsidy also modifies the evolution of $c(t)$, which was not the case with a lump sum redistribution (Appendix E.1).

Appendix F. Extensions

F.1. **Energy composite.** We consider final goods production

$$Y(t) = \theta_f K_f(t)^{\alpha_f} E(t)^{\mu_f + \nu_f} N_f(t)^{1-\alpha_f-\mu_f-\nu_f}\,,$$

where $E(t)$ is an energy composite variable defined by the CES function

$$E(t) = \left(\frac{\mu_f}{\mu_f+\nu_f} E_b(t)^r + \frac{\nu_f}{\mu_f+\nu_f} E_g(t)^r\right)^{\frac{1}{r}}\,,$$

with $r \in (-\infty, 1]$ and elasticity of substitution $1/(1-r)$. When $r = 0$, we recover the Cobb–Douglas production function used in the paper. We detrend all variables as usual and, from profit maximization, obtain the first-order conditions

$$\begin{aligned} r(t) &= \alpha_f y(t)/k_f(t)\,, \\ p_b(t)\, e_b(t) &= \mu_f \left(\frac{e_b(t)}{e(t)}\right)^r y(t)\,, \\ p_g(t)\, e_g(t) &= \nu_f \left(\frac{e_g(t)}{e(t)}\right)^r y(t)\,, \\ w(t) &= (1-\alpha_f-\mu_f-\nu_f) y(t)/n_f(t)\,. \end{aligned}$$

The production functions and first-order conditions in the brown and green energy sectors remain unchanged. When $r = 0$, we can aggregate all equations to obtain a single equation, $y(t) = \tilde{y} k(t)^{\alpha/\mu}$, with two unknowns $\{y(t), k(t)\}$ (see Appendix B.2). When $r \neq 0$, this aggregation is no longer possible, and we have a non-linear system of 11 equations with 12

unknowns $\{y(t), k(t), k_f(t), k_b(t), k_g(t), n_f(t), n_b(t), n_g(t), e(t), e_b(t), e_g(t), x(t)\}$. These equations consist of the production functions and combinations of the different first-order conditions

$$
\begin{aligned}
y(t) &= \theta_f k_f(t)^{\alpha_f} e(t)^{\mu_f+\nu_f} n_f(t)^{1-\alpha_f-\mu_f-\nu_f}\,,\\
e_b(t) &= \theta_b k_b(t)^{\alpha_b} x(t)^{\mu_b} n_b(t)^{1-\alpha_b-\mu_b}\,,\\
e_g(t) &= \theta_g k_g(t)^{\alpha_g} n_g(t)^{1-\alpha_g}\,,\\
e(t) &= \left(\frac{\mu_f}{\mu_f+\nu_f}\, e_b(t)^r + \frac{\nu_f}{\mu_f+\nu_f}\, e_g(t)^r\right)^{\frac{1}{r}}\,,\\
k_f(t) &= \frac{\alpha_f}{\alpha_f + \alpha_b\mu_f\left(\frac{e_b(t)}{e(t)}\right)^r + \alpha_g\nu_f\left(\frac{e_g(t)}{e(t)}\right)^r}\, k(t)\,,\\
k_b(t) &= \frac{\alpha_b\mu_f\left(\frac{e_b(t)}{e(t)}\right)^r}{\alpha_f + \alpha_b\mu_f\left(\frac{e_b(t)}{e(t)}\right)^r + \alpha_g\nu_f\left(\frac{e_g(t)}{e(t)}\right)^r}\, k(t)\,,\\
k_g(t) &= \frac{\alpha_g\nu_f\left(\frac{e_g(t)}{e(t)}\right)^r}{\alpha_f + \alpha_b\mu_f\left(\frac{e_b(t)}{e(t)}\right)^r + \alpha_g\nu_f\left(\frac{e_g(t)}{e(t)}\right)^r}\, k(t)\,,\\
n_f(t) &= \frac{1-\alpha_f-\mu_f-\nu_f}{1-\alpha_f-\mu_f-\nu_f + (1-\alpha_b-\mu_b)\mu_f\left(\frac{e_b(t)}{e(t)}\right)^r + (1-\alpha_g)\nu_f\left(\frac{e_g(t)}{e(t)}\right)^r}\,,\\
n_b(t) &= \frac{(1-\alpha_b-\mu_b)\mu_f\left(\frac{e_b(t)}{e(t)}\right)^r}{1-\alpha_f-\mu_f-\nu_f + (1-\alpha_b-\mu_b)\mu_f\left(\frac{e_b(t)}{e(t)}\right)^r + (1-\alpha_g)\nu_f\left(\frac{e_g(t)}{e(t)}\right)^r}\,,\\
n_g(t) &= \frac{(1-\alpha_g)\nu_f\left(\frac{e_g(t)}{e(t)}\right)^r}{1-\alpha_f-\mu_f-\nu_f + (1-\alpha_b-\mu_b)\mu_f\left(\frac{e_b(t)}{e(t)}\right)^r + (1-\alpha_g)\nu_f\left(\frac{e_g(t)}{e(t)}\right)^r}\,,\\
x(t) &= \frac{\mu_f\mu_b}{c_x}\left(\frac{e_b(t)}{e(t)}\right)^r y(t)\,.
\end{aligned}
$$

We observe that when $r \neq 0$, carbon intensity, defined as $\epsilon x(t)/y(t)$, is no longer constant across countries.

The household problem is exactly as in the paper (see Appendix B.3 for details)

$$
\begin{aligned}
\dot{k}(t) &= w(t) + (r(t) - (\delta + p(t)))k(t) - c(t)\,,\\
\frac{\dot{c}(t)}{c(t)} &= \frac{r(t) - (\delta+\rho)}{\sigma} - p(t)\,,
\end{aligned}
$$

where $r(t) = \alpha_f\, y(t)/k_f(t)$ and $w(t) = (1-\alpha_f-\mu_f-\nu_f)y(t)/n_f(t)$. Note that, from the above system of equations, we can easily obtain $w(t) + r(t)k(t) = y(t) - c_x x(t)$.

We can finally recast our equilibrium conditions into a MFG system, described in the following proposition.

Proposition 4 (MFG system with CES production)**.** *The competitive equilibrium with heterogeneous countries and a CES production function can be characterized by a system of nonlinear equations, two partial differential equations (PDEs) and two ordinary differential equations (ODEs). The system of* ***nonlinear equations*** *is*

$$\mathbf{F}(\mathbf{x}|k) = \mathbf{0}\,,$$

where $\mathbf{F} : \mathbb{R}^{11} \to \mathbb{R}^{11}$ *is a vector-valued function with* $\mathbf{x} = (y, k_f, k_b, k_g, n_f, n_b, n_g, e, e_b, e_g, x)^\intercal$*, and*

$$\mathbf{F}(\mathbf{x}|k) = \begin{pmatrix} y - \theta_f k_f^{\alpha_f} e^{\mu_f+\nu_f} n_f^{1-\alpha_f-\mu_f-\nu_f} \\ e_b - \theta_b k_b^{\alpha_b} x^{\mu_b} n_b^{1-\alpha_b-\mu_b} \\ e_g - \theta_g k_g^{\alpha_g} n_g^{1-\alpha_g} \\ e - \left(\frac{\mu_f}{\mu_f+\nu_f}\, e_b^r + \frac{\nu_f}{\mu_f+\nu_f}\, e_g^r\right)^{\frac{1}{r}} \\ k_f - \frac{\alpha_f}{\alpha_f+\alpha_b\mu_f\left(\frac{e_b}{e}\right)^r+\alpha_g\nu_f\left(\frac{e_g}{e}\right)^r}\, k \\ k_b - \frac{\alpha_b\mu_f\left(\frac{e_b}{e}\right)^r}{\alpha_f+\alpha_b\mu_f\left(\frac{e_b}{e}\right)^r+\alpha_g\nu_f\left(\frac{e_g}{e}\right)^r}\, k \\ k_g - \frac{\alpha_g\nu_f\left(\frac{e_g}{e}\right)^r}{\alpha_f+\alpha_b\mu_f\left(\frac{e_b}{e}\right)^r+\alpha_g\nu_f\left(\frac{e_g}{e}\right)^r}\, k \\ n_f - \frac{1-\alpha_f-\mu_f-\nu_f}{1-\alpha_f-\mu_f-\nu_f+(1-\alpha_b-\mu_b)\mu_f\left(\frac{e_b}{e}\right)^r+(1-\alpha_g)\nu_f\left(\frac{e_g}{e}\right)^r} \\ n_b - \frac{(1-\alpha_b-\mu_b)\mu_f\left(\frac{e_b}{e}\right)^r}{1-\alpha_f-\mu_f-\nu_f+(1-\alpha_b-\mu_b)\mu_f\left(\frac{e_b}{e}\right)^r+(1-\alpha_g)\nu_f\left(\frac{e_g}{e}\right)^r} \\ n_g - \frac{(1-\alpha_g)\nu_f\left(\frac{e_g}{e}\right)^r}{1-\alpha_f-\mu_f-\nu_f+(1-\alpha_b-\mu_b)\mu_f\left(\frac{e_b}{e}\right)^r+(1-\alpha_g)\nu_f\left(\frac{e_g}{e}\right)^r} \\ x - \frac{\mu_f\mu_b}{c_x}\left(\frac{e_b}{e}\right)^r y \end{pmatrix}.$$

The first PDE is a ***Hamilton–Jacobi–Bellman (HJB) equation***

$$\rho\, v(t,k) \;=\; \max_c \left\{ \mathrm{e}^{(1-\sigma)\int_0^t p(u)\mathrm{d}u}\, \frac{c^{1-\sigma}}{1-\sigma} - \frac{1}{1-\sigma} + \frac{\partial v}{\partial k}(t,k)\,(y(k) - c_x x(k) - (p(t)+\delta)\; k - c) + \frac{\partial v}{\partial t}(t,k) \right\},$$

where $(t,k) \in \mathbb{R}^+ \times \mathbb{R}^+$*, and* $y(k)$ *and* $x(k)$ *are obtained from* $\mathbf{F}(\mathbf{x}|k) = \mathbf{0}$*. We impose Cauchy boundary conditions*

$$v(t,0) = -\frac{1}{\rho(1-\sigma)}\,,\ \text{for } \sigma \in (0,1)\,, \quad v(t,0) = -\infty\,,\ \text{for } \sigma \geq 1\,, \quad \frac{\partial v}{\partial k}(t,0) = +\infty\,,$$

and terminal condition

$$\lim_{t\to+\infty} k\, \frac{\partial v}{\partial k}(t,k)\, e^{-\rho t} = 0\,.$$

The second PDE is a ***transport equation***

$$\frac{\partial u}{\partial t}(t,k) = -\frac{\partial}{\partial k}\left(i(t,k)\,u(t,k)\right)\,,$$

where $i(t,k) \coloneqq y(k) - c_x x(k) - (p(t)+\delta)\,k - \left(\frac{\partial v}{\partial k}(t,k)\right)^{-\frac{1}{\sigma}} \mathrm{e}^{\frac{1-\sigma}{\sigma}\int_0^t p(u)\mathrm{d}u}$*, where* $y(k)$ *and* $x(k)$ *are obtained from* $\mathbf{F}(\mathbf{x}|k) = \mathbf{0}$*, and with Dirichlet boundary conditions*

$$u(t,0) = 0\,, \quad u(t,\infty) = 0\,,$$

and initial condition

$$u(0,k) = u_0(k) \geq 0\,, \text{ with } \int_0^\infty u_0(k)\,\mathrm{d}k = 1\,.$$

Finally, the ODEs are the ***climate equations***

$$\left\{\begin{array}{rcl} \dot{s}(t) &=& \phi\,\bar{k}(t) - (p(t)+\psi)s(t)\,, \\ \dot{p}(t) &=& -\gamma\left(\frac{\phi\,\bar{k}(t)}{s(t)} - \psi\right)\,, \end{array}\right.$$

where $\bar{k}(t) \coloneqq \int_0^\infty \tilde{y}\,k^{\frac{\alpha}{\mu}}u(t,k)\,\mathrm{d}k$*, and with initial conditions*

$$s(0) = s_0 \geq 0\,, \quad p(0) = p_0\,.$$

Proof. Same proof as for Proposition 3. □

F.2. **International capital market.** In the paper (see Proposition 3), we assume that in each country, firms' capital $k(t)$ is equal to savings (or assets) $a(t)$. We instead consider here an international capital market with a world interest rate $r(t)$ clearing this market. Each country, however, faces a specific interest rate $\tilde{r}(t)$, which is related to the world interest rate but also depends negatively on its net foreign asset position $a(t) - k(t)$. Formally, we assume

$$\tilde{r}(t) = r(t)\,\mathrm{e}^{-\chi(a(t)-k(t))}\,,$$

where $\chi \geq 0$. This formulation is close to that used in small open economy models with a debt-elastic interest rate premium, as in Schmitt-Grohe and Uribe (2003). When optimizing, firms take $\tilde{r}(t)$ as given, which yields (see Appendix B for details)

$$\begin{aligned} \tilde{r}(t) &= \alpha\tilde{y}k(t)^{\frac{\alpha}{\mu}-1} \\ \Leftrightarrow a(t) &= k(t) + \frac{\ln\left(\frac{r(t)}{\alpha\tilde{y}}\right) + \frac{\mu-\alpha}{\mu}\ln k(t)}{\chi} \\ \Leftrightarrow a(t) &= F(k(t))\,. \end{aligned}$$

When $\theta_f(t,k) = \theta_{f0}$, $\tilde{y}$ does not depend on k, and we can easily show that $F(\cdot)$ is a bijective function with $\partial F(k(t))/\partial k(t) \geq 1$. When $\theta_f(t,k)$ depends on k (as is the case in our paper;

see Section 5.1), then $\tilde{y}$ also depends on k, and we are no longer certain that $F(\cdot)$ is always increasing in k and therefore bijective. Indeed, we can compute

$$\frac{\partial F(k)}{\partial k} = 1 + \frac{\mu - \alpha}{\mu\chi k} - \frac{2\,\theta_{f0}\,\beta_f\,\mathrm{e}^{-\beta_g t}\,\mathrm{e}^{-\beta_f(k-k_{\mu 0})}}{\mu\chi\,\theta_f(t,k)\left(1+\mathrm{e}^{-\beta_f(k-k_{\mu 0})}\right)^2}\,.$$

We can show that $F(\cdot)$ is increasing at the boundaries ($\lim_{k\to 0}\partial F(k)/\partial k = \infty$ and $\lim_{k\to\infty}\partial F(k)/\partial k = 1$), but that, for instance, when $k = k_{\mu 0}$, we obtain

$$\frac{\partial F(k)}{\partial k} = 1 + \frac{\mu - \alpha}{\mu\chi\,k_{\mu 0}} - \frac{\beta_f\,\mathrm{e}^{-\beta_g t}}{2\,\mu\chi}\,,$$

whose sign is ambiguous. To ensure that this expression is positive for all t and χ, we must impose the condition $(\alpha-\mu)/k_{\mu 0} > \beta_f/2$. This is a necessary condition (for the case $k = k_{\mu 0}$), but we cannot prove analytically that it is a sufficient condition ensuring that $\partial F(k)/\partial k$ is positive for all k. In the remaining of this appendix, we therefore assume that the function $F(\cdot)$ is bijective.

We observe that when $\chi \to 0$, $a(t) = k(t)$ and the model reduces to that studied in the paper (see Proposition 3). When $\chi = 0$, all countries choose the same level of capital (and hence have the same level of production), implying that the distribution of capital across countries is degenerate.

The household's budget constraint is

$$\dot{a}(t) = w(t) + (\tilde{r}(t) - (p(t) + \delta))\,a(t) - c(t)\,.$$

Therefore, in the model with international capital market, the state variable is assets $a(t)$, whose distribution is characterized by $u(t,a)$, with $u_0(a) \coloneqq u(0,a)$ given. The distribution of capital across countries is denoted by $u_k(t,k)$ and is given by (see Appendix C.3 for details)

$$u_k(t,k) = u(t,F(k))\frac{\partial F(k)}{\partial k}\,.$$

Finally, the world interest rate $r(t)$ adjusts to clear the international capital market, such that

$$\int_0^\infty a\,u(t,a)\,\mathrm{d}a = \int_0^\infty k\,u_k(t,k)\,\mathrm{d}k\,.$$

The above equation can be rewritten as

$$\ln r(t) = \ln \alpha\tilde{y} - \frac{\mu-\alpha}{\mu}\,\mathbb{E}\left[\ln k(t)\right]\,,$$

which shows that, at the steady state, we obtain $r^* = \rho + \delta$ as before.

We can now recast all our equilibrium conditions into a single MFG system, described in the following proposition.

Proposition 5 (MFG system with international capital market)**.** *The competitive equilibrium with heterogeneous countries and international capital market can be characterized by a system of one nonlinear equation, two partial differential equations (PDEs), one market clearing condition, and two ordinary differential equations (ODEs). The* ***nonlinear equation*** *is*

$$a = F(k)\,,$$

where

$$F(k) = k + \frac{\ln\left(\frac{r(t)}{\alpha\tilde{y}}\right) + \frac{\mu-\alpha}{\mu}\ln k}{\chi}\,,$$

is a bijective function.

The first PDE is a ***Hamilton–Jacobi–Bellman (HJB) equation***

$$\begin{aligned}\rho\, v(t,a) \;&= \max_{c}\left\{ \mathrm{e}^{(1-\sigma)\int_0^t p(u)\mathrm{d}u}\,\frac{c^{1-\sigma}}{1-\sigma} - \frac{1}{1-\sigma} + \right.\\ &\left.\frac{\partial v}{\partial a}(t,a)\left((\mu-\alpha)\,\tilde{y}\,\left(F^{-1}(a)\right)^{\frac{\alpha}{\mu}} + \left(r(t)\,\mathrm{e}^{-\chi\left(a-F^{-1}(a)\right)} - (p(t)+\delta)\right)\,a - c\right) + \frac{\partial v}{\partial t}(t,a)\right\}\,,\end{aligned}$$

where $(t,a)\in\mathbb{R}^+\times\mathbb{R}^+$*. We impose Cauchy boundary condition*

$$\frac{\partial v}{\partial a}(t,0) \geq \mathrm{e}^{(1-\sigma)\int_0^t p(u)\mathrm{d}u}\left((\mu-\alpha)\,\tilde{y}\,\left(F^{-1}(0)\right)^{\frac{\alpha}{\mu}}\right)^{-\sigma}\,,$$

and terminal condition

$$\lim_{t\to+\infty} a\,\frac{\partial v}{\partial a}(t,a)\,e^{-\rho t} = 0\,.$$

The second PDE is a ***transport equation***

$$\frac{\partial u}{\partial t}(t,a) = -\,\frac{\partial}{\partial a}\left(i(t,a)\,u(t,a)\right)\,,$$

where

$$\begin{aligned}i(t,a) \coloneqq&(\mu-\alpha)\,\tilde{y}\,\left(F^{-1}(a)\right)^{\frac{\alpha}{\mu}} + \left(r(t)\,\mathrm{e}^{-\chi\left(a-F^{-1}(a)\right)} - (p(t)+\delta)\right)\,a\\ &-\left(\frac{\partial v}{\partial a}(t,a)\right)^{-\frac{1}{\sigma}}\mathrm{e}^{\frac{1-\sigma}{\sigma}\int_0^t p(u)\mathrm{d}u}\,,\end{aligned}$$

and with Dirichlet boundary conditions

$$u(t,0) = 0\,,\quad u(t,\infty) = 0\,,$$

and initial condition

$$u(0,a) = u_0(a) \geq 0\,,\ \textit{with}\ \int_0^\infty u_0(a)\,\mathrm{d}a = 1\,.$$

The ***market clearing condition*** *is*

$$\int_0^\infty a\,u(t,a)\,\mathrm{d}a = \int_0^\infty k\,u(t,F(k))\,\frac{\partial F(k)}{\partial k}\,\mathrm{d}k\,.$$

Finally, the ODEs are the ***climate equations***

$$\left\{ \begin{array}{rcl} \dot{s}(t) & = & \phi\, \bar{k}(t) - (p(t) + \psi) s(t)\,, \\ \dot{p}(t) & = & -\gamma \left(\frac{\phi\, \bar{k}(t)}{s(t)} - \psi \right)\,, \end{array} \right.$$

where $\bar{k}(t) \coloneqq \int_0^\infty \tilde{y}\, k^{\frac{\alpha}{\mu}}\, u(t, F(k))\, \frac{\partial F(k)}{\partial k}\, \mathrm{d}k$*, and with initial conditions*

$$s(0) = s_0 \geq 0\,, \quad p(0) = p_0\,.$$

Proof. Same proof as for Proposition 3. To determine the Cauchy condition of the HJB problem, we first note that the first order condition with respect to c also holds when $a = 0$, that is

$$\frac{\partial v}{\partial a}(t, 0) = \mathrm{e}^{(1-\sigma) \int_0^t p(u) \mathrm{d}u} \left(c(a = 0) \right)^{-\sigma}\,.$$

Then, when $a = 0$, we must impose $\dot{a} \geq 0$ to rule out negative assets, that is

$$(\mu - \alpha)\, \tilde{y}\, \left(F^{-1}(0) \right)^{\frac{\alpha}{\mu}} \geq c(a = 0)\,.$$

From the concavity of the utility function ($\sigma > 0$), we finally obtain as boundary condition

$$\frac{\partial v}{\partial a}(t, 0) \geq \mathrm{e}^{(1-\sigma) \int_0^t p(u) \mathrm{d}u} \left((\mu - \alpha)\, \tilde{y}\, \left(F^{-1}(0) \right)^{\frac{\alpha}{\mu}} \right)^{-\sigma}\,.$$

□

At the steady state (represented by *), the link between the interest rate $\tilde{r}_t$ and the net foreign asset position $nfa(t) = a(t) - k(t)$ is

$$\left. \frac{\partial \tilde{r}_t}{\partial\, nfa(t)} \right|_* = -\chi\, r(t)\, \mathrm{e}^{-\chi\, nfa(t)} \big|_* = -\chi\, r* = -\chi\, (\delta + \rho)\,.$$

Let us consider the effect of an increase in $nfa(t)$ corresponding to $z\%$ of the steady state of annual output, that is $\Delta nfa(t) = z/100 \times \tilde{y}\, (k^*)^{\alpha/\mu}\, /32$. Then $\tilde{r}_t$ falls by $\Delta \tilde{r}_t = \chi\, (\delta + \rho)\, \Delta nfa(t)$. Expressing the fall in $\tilde{r}_t$ in annual terms gives $\Delta^{ann} \tilde{r}_t \approx \Delta \tilde{r}_t / 32$.

BANQUE CENTRALE DU LUXEMBOURG

EUROSYSTÈME

2, boulevard Royal
L-2983 Luxembourg

Tél.: +352 4774-1
Fax: +352 4774 4910

www.bcl.lu • info@bcl.lu